Theoretical investigations on lattice Boltzmann method: an amended MBD and improved LBM

Journal:	*Acta Mechanica Sinica*
Manuscript ID	ams2021-266
Manuscript Type:	Full Length Paper
Date Submitted by the Author:	20-May-2021
Complete List of Authors:	Xing, Jing Tang; University of Southampton, Maritime Eng, SES, FEPS
Keywords:	Amended Maxwell-Boltzmann distribution, Improved LBM, Macroscopic internal energy, Conservation laws from LBE, Lagrangian multiplier method


Acta
Mechanica
Sinica
Springer

Theoretical investigations on lattice Boltzmann method: *an amended MBD and improved LBM*

Jing Tang Xing

Maritime Engineering, School of Engineering, FEPS, University of Southampton, Southampton, UK

Abstract
This paper presents theoretical investigations of lattice Boltzmann method (LBM) to develop a completed LBM theory. Based on H-theorem with Lagrangian multiplier method, an amended theoretical equilibrium distribution function (EDF) is derived, which modifies the current Maxwell-Boltzmann distribution (MBD) to include the total internal energy as its parameter. This modification allows the three conservation laws derived directly from lattice Boltzmann equation (LBE) without additional small-parameter expansions adopted in references. From this amended theoretical EDF an improved LBM is developed, in which the total internal energy like the mass density and mean velocity is a new macroscopic variable to be updated for different times and cells during simulations. The developed method provides a means to consider external forces and energy generation sources as generalised forces in LBM simulations. The corresponding model and implementation process of the improved LBM are presented with its performance theoretically investigated. Analytically hand-workable examples are given to illustrate its applications and to confirm its validity. The paper will excite more researchers and scientists of this area to numerically practice the new theory and method dealing with complex physical problems, from which it is expected to further advance LBM benefiting science and engineering.

Key Words: Amended Maxwell-Boltzmann distribution, Improved LBM, Macroscopic internal energy, Conservation laws from LBE, Lagrangian multiplier method.

1. Introduction

LBM is based on microscopic molecule dynamics [1-5], concerning molecule distribution in space. Boltzmann transport equation (BTE) [6-9] and H theorem confirms that the EDF is MBD [7], contributed a way to understand macroscopic world and from a mesoscopic method dealing with macroscopic motions [10-12]. The solution of BTE is very difficult, and attempts have been made to simplify the collision term, for which the best-known model [13] has been implemented. LBM was developed from the lattice gas automata (LGA) [14-15]. McNamara & Zanetti [16] contributed a historic contribution to replace the Boolean variable in LGA by a real variable, and initially created LBM. The idea of LBM is imaging gases / fluids as a finite number of particles with random motions, and their exchange of momentum and energy achieved through particle streaming and collisions. Key historic publications [13-63] making LBM into new stages should be highlighted. The important review papers [39, 59-81] and the influence books [82-97] have been published. LBM is considered as an effective method to model some phenomena not easily macroscopically described by other method [98]. It has many computer codes of LBM provided [85-87, 91, 99, 100].

In practical simulations based on the current LBM, it has been realized that it is probably most suitable for isothermal weakly-compressible flows. For complex flows, especially the ones involving high speed and large compressibility and obvious energy exchanges, it has suffered from numerical problems on accuracy, efficiency, and stability. To solve these problems, when simulating multicomponent flows, Swift et al [101,102] added an additional term of free energy in EDF for the conservation of total energy, including the surface, kinetic and internal energies to be satisfied [103]. Meanwhile, studying thermodynamics in incompressible limit, He et al [104] proposed a thermal model with an internal energy density distribution expressed by a multiplication of MBD and kinetic energy, so that the evolution equation of the introduced energy distribution together with original BTE were solved to simulate temperature fields. Until now, many recent publications, such as [105-112], still tried to add some numerical techniques, such as correctly resolve energy equation, high-order lattices, double distribution functions, hybrid LBM with finite difference or finite volume approaches etc., but nobody has deeply asked if there exist some fundamental theoretical incompleteness of the current LBM model. In the history of science advances, to solve a difficult problem reported by practices, it is not only to seek some technique-modifications on it, but also, more importantly, to check the original theory and physical mechanism of the problem to find if there is its inherent theoretical incompleteness. Based on this consideration, author through carefully reading the publications of LBM concerning its original principles and basic physical mechanism has found its following theoretical problems. We know that the background of LBM is the kinetic theory and BTE developed by studying the distribution of molecules of *ideal dilute gases*. Theoretical EDF obtained is MBD, in which three macroscopic variables: mass density, velocity and temperature T with Boltzmann constant K are the parameters. In this EDF, the KT reflecting the bulk energy was derived only by the state equation of gas [6], but not concerning other types of energy, such as the work done by viscous stress and the one caused by the gradient of mass density. Therefore, the momentum and energy conservation equations derived from MBD do not include the contribution from the full stress tensor in continuum mechanics, and there is not a term in the energy conservation equation concerning the contribution of external energy generation sources. Physical flows in continuum mechanics are governed by three conservation laws, of which the three variables, the mass density, velocity, and internal energy are key parameters. When we study macroscopic flows from a viewpoint of statistical mechanics, it should have a corresponding inherent theoretical EDF including these three key parameters to allow the three conservation laws to be derived from it. Therefore, this paper intends to tackle these important theoretical problems to develop an improved theory with amended LBM model, aiming for readers to follow in practical simulations to solve the mentioned difficulties of the current LBM.

The paper is a theoretical document written exactly based on the famous Boltzmann H-theorem [6] of the statistical mechanics, the laws of continuum mechanics [113-115], the energy flow theory [116-120], and the variational method in mathematical analysis. ***Section*** 1 from reading historical publications reveals the existing problems of LBM theory, that is the total internal energy is not involved in current EDF causing some theoretical and numerical problems. Sub-sections 2.1-2.3 derive the fundamental equations from continuum mechanics, which is used in sub-section 2.4 to develop an amended theoretical EDF including internal energy as a parameter, that is new contribution of the paper, and ***section*** 2 is a base of demonstrations in section 3 and 4. ***Section*** 3 demonstrates three conservation laws directly from the amended EDF with no small parameter expansions adopted in references. ***Section*** 4 gives the modified LBM based on the developed EDF with mass density, mean velocity and internal energy as parameters to be updated in numerical process. The formulations on generalised forces contributed by external forces and energy generation sources are provided and the implementation process of the improved method with its performance study are given. ***Section*** 5 gives some hand-workable examples by analysis to confirm the valid of theory and to illustrate applications.

2. Internal energy and amended theoretical EDF

To develop an amended theoretical EDF based on MBD function by introducing the total internal energy density as a macroscopic parameter, the knowledge in continuum mechanics including the state equation, material derivatives, Cauchy tress tensor, stress power, internal mechanical energy and its time / space derivatives with their statistical averages are required, which are discussed in this section.

2.1 Ideal gases, state equation and average internal thermal energy (AITE)

For ideal gases in the volume Ω containing N molecule particles, the state pressure p is defined by the equation of state in association with the Boltzmann constant k in the form [6]

$$p = \frac{NkT}{\Omega} = nkT, \qquad n = \frac{N}{\Omega}, \tag{2-1.1}$$

from which, we know that if the temperature T is a constant, the particle density is a function of the volume and affects the state pressure per individual particle by

$$\hat{p} = \frac{p}{n} = kT. \tag{2-1.2}$$

Physically, the dimension of the state pressure per individual particle is the pressure over the mass density, i.e., $\mathrm{Nm}^{-2}/(\mathrm{kg}m^{-3}) = (\mathrm{m/s})^2$ that is *a square of the instant velocity*, equaling the derivative of the pressure with respect to the mass density.

Huang [6] presented the detailed calculation of AITE based on EDF, and obtained the average thermal energy $\hat{e}$ of a particle

$$p = nkT = \frac{2}{3}n\hat{e}, \qquad \hat{e} = \frac{3kT}{2}, \tag{2-1.3}$$

where the pressure p and the temperature T are the physically measured quantities, from which AITE of the particles per unit volume is

$$\tilde{e} = n\hat{e} = \frac{3nkT}{2}. \tag{2-1.4}$$

From Eq. 2-1.2 *we may understand that the average internal energy, $\hat{e}$, as the square of averaged velocity of sound in the fluid.*

2.2 Cauchy tress tensor, power, and average internal mechanical energy (AIME)

In the continuum mechanics, using Cartesian tensor notations, see for examples, [113-115], the Cauchy stress tensor of fluids is given by

$$\sigma_{ij} = -p\delta_{ij} + \tilde{\sigma}_{ij}\ , \qquad \tilde{\sigma}_{ij} = 2\mu\left(V_{ij} - \frac{V_{ll}\delta_{ij}}{3}\right), \quad V_{ij} = \frac{v_{i,j} + v_{j,i}}{2}, \tag{2-2.1}$$

where p is the pressure caused by fluid flows, μ is the coefficient of viscosity, V_{ij} is deformation rate tensor, and $\tilde{\sigma}_{ij} = \tilde{\sigma}_{ji}$ denotes a symmetrical viscous stress tensor with $\tilde{\sigma}_{jj} = 0$, If the fluid is incompressible, the fluid dilation vanishes, $\partial v_l/\partial x_l = V_{ll} = 0$, the stress tensor reduces to

$$\sigma_{ij} = -p\delta_{ij} + 2\mu V_{ij}\ . \tag{2-2.2}$$

The power of stress per unit volume is given by $\sigma_{ij}V_{ij}$, which is a measured quantity. The internal mechanical energy of the fluid per unit mass can be obtained by integration from its reference state “0” to its current state “t”

$$\psi = \int_0^t \frac{\sigma_{ij}}{\rho} V_{ij}\mathrm{d}t, \qquad \frac{\mathrm{D}\psi}{\mathrm{D}t} = \frac{\sigma_{ij}}{\rho} V_{ij.} \tag{2-2.3}$$

Following the discussion on AITE per unit particle above, we can obtain AIME $\hat{\psi}$ per unit particle in a similar form as given in Eq. 2-1.3, i.e.

$$\hat{\psi} = \langle\psi\rangle = \frac{3}{2}\psi, \qquad \frac{\mathrm{D}\hat{\psi}}{\mathrm{D}t} = \langle\frac{\mathrm{D}\psi}{\mathrm{D}t}\rangle = \langle\frac{\sigma_{ij}}{\rho} V_{ij.}\rangle = \frac{\langle\sigma_{ij}V_{ij}\rangle}{n}\ , \tag{2-2.4}$$

which $\hat{\psi}$ has the dimension of pressure $\hat{p}$ per unit particle shown in Eq. 2.1.1. As a result of this, AIME of the particles per unit volume and its time derivative can be given by

$$\tilde{\psi} = n\hat{\psi} = \frac{3n}{2}\psi, \qquad \frac{\mathrm{D}\tilde{\psi}}{\mathrm{D}t} = n\frac{\mathrm{D}\hat{\psi}}{\mathrm{D}t} = \langle\sigma_{ij}V_{ij}\rangle, \tag{2-2.5}$$

from which with Eq. 2-2.3, it follows that the time change rate of AIME of the particles per unit volume is

$$\frac{\mathrm{D}\tilde{\psi}}{\mathrm{D}t} = \frac{3n\mathrm{D}\psi}{2\mathrm{D}t} = \sigma_{ij}u_{i,j}. \tag{2-2.6}$$

Here $()_{,j} = \partial()/\partial x_j$, as used in tensor analysis [113-115], the $\sigma_{ij}u_{i,j}$ is understood as the averaged one, although the same stress notations are adopted.

2.3 Material derivatives and gradient of internal mechanical energy per unit volume

A material point marked by its original position coordinate X_j moves in the space, and it arrives the position $x_i = (X_j, t)$ at time t, so that its velocity $v_i = (\partial x_i/\partial t)_X$ and acceleration $a_i = (\partial v_i/\partial t)_X$ where the subscript X implies the derivatives with respect to time t are taken for the same material point. This time derivative is called as a material derivative [113-115]. In continuum mechanics, the Eulerian description of motion represents motion quantities in $()(x_i, t)$ as functions of spatial position and time, which may be a scalar, vector, or tensor function. In the Eulerian description of motion, the material derivative is

$$\mathrm{D}()/\mathrm{D}t = \partial()/\partial t + (dx_i/dt)_X\,\partial()/\partial x_i = \partial()/\partial t + v_i\,\partial()/\partial x_i. \tag{2-3.1}$$

For a set of material points in a volume Ω with its surface S in the space at time t, the total quantity () of this set of particles is

$$I(\mathrm{t}) = \int_{\Omega(t)} ()\mathrm{d}\Omega\ , \tag{2-3.2}$$

where volume Ω is also a function of time due to the motion. The material derivative of the quantity I(t) is

$$\frac{\mathrm{D}I(t)}{\mathrm{D}t} = \frac{\mathrm{D}}{\mathrm{D}t}\int_{\Omega(t)} ()\mathrm{d}\Omega = \int_\Omega \frac{\partial()}{\partial t}\mathrm{d}\Omega + \int_S\ ()v_i v_i\,\mathrm{d}S\ , \tag{2-3.3}$$

where, physically, on the right-hand side the first integration denotes the time change rate of the quantity in the fixed volume, while the second one is caused by the boundary motion. Using the Green theorem [113-115], we can re-write above equation as

$$\frac{\mathrm{D}I(t)}{\mathrm{D}t} = \int_\Omega \left\{\frac{\partial()}{\partial t} + \frac{\partial[()v_i]}{\partial x_i}\right\}\mathrm{d}\Omega = \int_\Omega \left\{\frac{\partial()}{\partial t} + ()\frac{\partial v_i}{\partial x_i}\right\}\mathrm{d}\Omega. \tag{2-3.4}$$

Introducing the mass density ρ and the mass conservation equation, we obtain

$$\frac{\mathrm{D}}{\mathrm{D}t}\int_{\Omega} \rho()\mathrm{d}\Omega = \int_{\Omega} \rho\frac{\mathrm{D}()}{\mathrm{D}t}\mathrm{d}\Omega. \tag{2-3.5}$$

2.3.1 Gradient of internal mechanical energy per unit volume in equilibrium state

The gradient of the internal mechanical energy per unit volume in equilibrium state can be derived by using Fig. 1, in which a volume element $\Delta\Omega$ closed by surface ΔS of unit normal vector ν_i pointing from inside to outside of the volume is in its equilibrium state, so that it satisfies the equilibrium equation

Figure 1

Fig. **1** The gradient of internal mechanical energy.

$$\sigma_{ij,j} + f_i = 0, \tag{2-3.6}$$

$$\int_{\Delta\Omega} \sigma_{ij,j}\mathrm{d}\Omega + \int_{\Delta\Omega} f_i\mathrm{d}\Omega = \int_{\Delta S} \sigma_{ij}\nu_j\mathrm{d}S + \int_{\Delta\Omega} f_i\mathrm{d}\Omega = \int_{\Delta S} \sigma_{ij}\nu_j\mathrm{d}S + \Delta\Omega f_i = 0,$$

where f_i is the body force per unit volume. When the volume tends zero, the resultant force at a point vanishes

$$T_R = \int_{\Delta S}\sigma_{ij}\nu_j\mathrm{d}S = 0. \tag{2-3.7}$$

The change of internal energy per unit volume is calculated by the work done by the stress in the gradient $\Delta U_{i,j}$ of displacement field $U_i$in the form

$$\Delta(n\psi) = \sigma_{ij}\Delta U_{i,j}, \tag{2-3.8}$$

from which, when integrated over the volume $\Delta\Omega$, and then using the Green theorem, it follows

$$\int_{\Delta\Omega} \Delta(n\psi)\mathrm{d}\Omega = \int_{\Delta\Omega}\sigma_{ij}\Delta U_{i,j}\mathrm{d}\Omega = \int_{\Delta S}\sigma_{ij}\Delta U_i\nu_j\,\mathrm{d}S - \int_{\Delta\Omega}\sigma_{ij,j}\Delta U_i\mathrm{d}\Omega. \tag{2-3.9}$$

Since the volume is very small, we approximate the displacement as the one at the central point, therefore, based on Eq. 2-3.7 in equilibrium state, we obtain the gradient of the internal mechanical energy per unit volume as

$$\int_{\Delta\Omega} \Delta(n\psi)\mathrm{d}\Omega = \Delta U_i\int_{\Delta S}\sigma_{ij}\nu_j\,\mathrm{d}S - \int_{\Delta\Omega}\sigma_{ij,j}\Delta U_i\mathrm{d}\Omega = -\int_{\Delta\Omega}\sigma_{ij,j}\Delta U_i\mathrm{d}\Omega, \tag{2-3.10}$$

$$\Delta(n\psi) = -\sigma_{ij,j}\Delta U_i, \qquad \frac{\Delta(n\psi)}{\Delta U_i} = -\sigma_{ij,j}\ , \qquad \frac{\partial(n\psi)}{\partial x_i} = -\sigma_{ij,j}\ ,$$

where we have introduced $x_i = X_i + U_i$, and the particle displacement increment $\Delta U_i = \Delta x_i$.

2.3.2 Time change rate of AIME per unit volume in equilibrium state

The time change rate of AIME per unit volume in the equilibrium state can be derived from the principle of virtual power. Since the system is in equilibrium state, there is no power exchange with outside, so that the summation of the stress power and the time change rate of AIME per unit volume vanishes

$$-\int_{\Delta S}\sigma_{ij}u_i\nu_j\mathrm{d}S = \frac{\mathrm{D}}{\mathrm{D}t}\int_{\Delta\Omega}\tilde{\psi}\mathrm{d}\Omega = \int_{\Delta\Omega}\frac{3n\mathrm{D}\psi}{2\mathrm{D}t}\mathrm{d}\Omega, \tag{2-3.11}$$

from which, when the Green theorem used, it follows

$$-\int_{\Delta\Omega}(\sigma_{ij}u_i)_{,j}\mathrm{d}\Omega = \int_{\Delta\Omega}\frac{3n\mathrm{D}\psi}{2\mathrm{D}t}\mathrm{d}\Omega. \tag{2-3.12}$$

Since the volume $\Delta\Omega$ is arbitrary, we have

$$\frac{3n\mathrm{D}\psi}{2\mathrm{D}t} = -(\sigma_{ij}u_i)_{,j} = q_{j,j}, \tag{2-3.13}$$

where q_j is defined as the averaged energy flow-density vector [116-117]

2.3.3 Equation satisfied by the internal mechanical energy per unit mass

The equilibrium equation of power denoted by the internal mechanical energy per unit mass in the equilibrium state is obtained by investigating Eq. 2-3.11, which, when the material derivative Eq. 2-3.4 used, becomes

$$\int_{\Delta S}\sigma_{ij}v_i v_j \mathrm{d}\hat{S} = \frac{\mathrm{D}}{\mathrm{D}t}\int_{\Delta\Omega}\psi \mathrm{d}\Omega = \int_{\Delta\Omega}\left(\frac{\mathrm{D}\psi}{\mathrm{D}t} + \psi v_{i,i}\right)\mathrm{d}\Omega = \int_{\Delta\Omega}\left(\frac{\sigma_{ij}V_{ij}}{\rho} + \psi v_{i,i}\right)\mathrm{d}\Omega, \tag{2-3.14}$$

where "^" is to identify the quantity involving the ones for unit mass only. As a result of this, and when the Green theorem used, it follows

$$\int_{\Delta\Omega}(\sigma_{ij}v_i)_{,j}\mathrm{d}\hat{\Omega} = \int_{\Delta\Omega}(\sigma_{ij}v_i)_{,j}\frac{\mathrm{d}\Omega}{\rho} = \int_{\Delta\Omega}\left(\frac{\sigma_{ij}V_{ij}}{\rho} + \psi v_{i,i}\right)\mathrm{d}\Omega, \tag{2-3.15}$$

where $d\hat{\Omega}$ denotes the volume element per unit mass equaling $\frac{\mathrm{d}\Omega}{\rho}$. Therefore, from Eq. 2-3.15, we have

$$\frac{\sigma_{ij}V_{ij}}{\rho} + \psi v_{i,i} = -\frac{q_{j,j}}{\rho}, \qquad \sigma_{ij}V_{ij} + n\psi v_{i,i} + q_{j,j} = 0, \tag{2-3.16}$$

where the mass density is replaced by the particle density n.

2.4 Boltzmann H-theorem and amended theoretical EDF

The famous MBD function was derived for ideal gases with its AITE in the form $\tilde{e} = 3nkT/2$ [6], therefore, the momentum and energy conservation equations derived from MBD function does not include the contribution from the stress tensor in continuum mechanics. As mentioned in introduction, for simulating complex thermodynamic and multicomponent flows, etc., several *technique modifications* [101-112] were proposed to deal with some numerical issues met in their practices, but it has not solved the theoretical incompleteness of the current theory.

As discussed in subsection 2.2, we have introduced an AIME per unit volume and per unit particle based on the theory of continuous mechanics and statistical average, which are summarized in the forms

$$\begin{gathered} e = \widetilde{K} + \tilde{\varepsilon}, \quad \tilde{\varepsilon} = \tilde{e} + \tilde{\psi} \quad \hat{\varepsilon} = \hat{e} + \hat{\psi} = 3\bar{T}/2, \\ \widetilde{K} = n\widehat{K}, \quad \tilde{e} = n\hat{e}, \quad \tilde{\psi} = n\hat{\psi}, \\ \widehat{K} = u_i u_i/2\ , \quad \hat{e} = 3kT/2, \quad \hat{\psi} = 3\psi/2, \end{gathered} \tag{2-4.1}$$

where e denotes the total internal energy per unit volume, which consists of the kinetic one $\widetilde{K}$ and the thermal mechanical one $\tilde{\varepsilon}$ equaling a summation of the thermal one $\tilde{e}$ and the mechanical one $\tilde{\psi}$. The hats "^" denote the corresponding variables per unit particle. These averaged internal energies are macroscopic quantities being the functions of position x_i and time t.

Based on the developed AIME and the Boltzmann's H theorem [6], we can derive the amended theoretical EDE. We can conclude that EDF $f_0(\boldsymbol{x},\boldsymbol{v},t)$ in a volume Ω for a prescribed density n , mean momentum $n\boldsymbol{u}$, and energy per unit volume $ne = 0.5n\mathbf{u}\cdot\mathbf{u} + \tilde{\varepsilon}$, $\tilde{\varepsilon} = 1.5n(KT+\psi) = 1.5n\bar{T}$ minimizes the H functional

$$H(t) = \int f(\boldsymbol{x},\boldsymbol{v},t)\log[f(\boldsymbol{x},\boldsymbol{v},t)]\mathrm{d}\Omega\mathrm{d}V, \tag{2-4.2}$$

where $\mathrm{d}V = \mathrm{d}v_1\mathrm{d}v_2\mathrm{d}v_3$ is the differential volume element of the velocity space. We require that the mass, momentum, and energy of this particle system in the volume Ω are conservative, i.e.

$$n\Omega = \int f(\boldsymbol{x},\boldsymbol{v},t)\,\mathrm{d}\Omega\mathrm{d}V, \quad n\boldsymbol{u}\Omega = \int \boldsymbol{v}f(\boldsymbol{x},\boldsymbol{v},t)\,\mathrm{d}\Omega\mathrm{d}V, \quad ne\Omega = \int 0.5(\boldsymbol{v}\cdot\boldsymbol{v})f(\boldsymbol{x},\boldsymbol{v},t)\,\mathrm{d}\Omega\mathrm{d}V, \tag{2-4.3}$$

which are the constrains of the H functional. Using the Lagrangian multiplier method [99], introducing two scalar multipliers λ_1 and λ_3 , and a vector one $\boldsymbol{\lambda}_2$ to release the variational constrains in Eq. 2-4.3 of the functional in Eq.2-4.2, we obtain the new functional

$$\begin{gathered} \widetilde{H}(f,\lambda_1,\boldsymbol{\lambda}_2,\lambda_3) = \int f(\boldsymbol{x},\boldsymbol{v},t)\log[f(\boldsymbol{x},\boldsymbol{v},t)]\mathrm{d}\Omega\mathrm{d}V - \lambda_1\left[n\Omega - \int f(\boldsymbol{x},\boldsymbol{v},t)\,\mathrm{d}\Omega\mathrm{d}V\right] \\ -\boldsymbol{\lambda}_2\cdot\left[\boldsymbol{nu\Omega} - \int \boldsymbol{v}f(\boldsymbol{x},\boldsymbol{v},t)\,\mathrm{d}\Omega\mathrm{d}V\right] - \lambda_3\left[ne\Omega - \int 0.5(\boldsymbol{v}\cdot\boldsymbol{v})f(\boldsymbol{x},\boldsymbol{v},t)\,\mathrm{d}\Omega\mathrm{d}V\right]. \end{gathered} \tag{2-4.4}$$

The variation of the functional $\widetilde{H}$ gives

$$\begin{gathered} \delta\widetilde{H} = \int \delta f[1 + \log f + \lambda_1 + \boldsymbol{\lambda}_2\cdot\boldsymbol{v} + 0.5\lambda_3(\boldsymbol{v}\cdot\boldsymbol{v})]\,\mathrm{d}\Omega\mathrm{d}V - \delta\lambda_1\left[n\Omega - \int f(\boldsymbol{x},\boldsymbol{v},t)\,\mathrm{d}\Omega\mathrm{d}V\right] \\ -\delta\boldsymbol{\lambda}_2\cdot\left[n\boldsymbol{u}\Omega - \int \boldsymbol{v}f(\boldsymbol{x},\boldsymbol{v},t)\,d\Omega dV\right] - \delta\lambda_3\left[ne\Omega - \int 0.5(\boldsymbol{v}\cdot\boldsymbol{v})f(\boldsymbol{x},\boldsymbol{v},t)\,d\Omega dV\right], \end{gathered} \tag{2-4.5}$$

from which, when $\delta\widetilde{H} = 0$, it yields the constrain conditions in Eq. 2-4.3 and the equation

$$[1 + logf + \lambda_1 + \boldsymbol{\lambda}_2 \cdot \boldsymbol{v} + 0.5\lambda_3(\boldsymbol{v}\cdot\boldsymbol{v})] = 0. \tag{2-4.6}$$

The solution of Eq. 2-4.6 is EDF satisfying the conservative constrains in Eq. 2-4.3, which is

$$f_0 = \exp\left[-1 - \lambda_1 + \frac{\boldsymbol{\lambda}_2\cdot\boldsymbol{\lambda}_2}{2\lambda_3} - \frac{\lambda_3}{2}\left(\frac{\boldsymbol{\lambda}_2}{\lambda_3} + \boldsymbol{v}\right)\cdot\left(\frac{\boldsymbol{\lambda}_2}{\lambda_3} + \boldsymbol{v}\right)\right], \tag{2-4.7}$$

where, we have introduced the equality

$$\boldsymbol{\lambda}_2 \cdot \boldsymbol{v} + 0.5\lambda_3(\boldsymbol{v}\cdot\boldsymbol{v}) = -\frac{\boldsymbol{\lambda}_2\cdot\boldsymbol{\lambda}_2}{2\lambda_3} + \frac{\lambda_3}{2}\left(\frac{\boldsymbol{\lambda}_2}{\lambda_3} + \boldsymbol{v}\right)\cdot\left(\frac{\boldsymbol{\lambda}_2}{\lambda_3} + \boldsymbol{v}\right) \tag{2-4.8}$$

We consider a new set of Lagrangian multipliers $d, \boldsymbol{\beta}, \gamma$ from which the EDF is represented in the standard form

$$f_0 = d\exp\left[-\frac{(\boldsymbol{v}-\boldsymbol{\beta})\cdot(\boldsymbol{v}-\boldsymbol{\beta})}{\gamma}\right], \tag{2-4.9}$$

which satisfies the conservative laws

$$\begin{gathered} n\Omega = \int f_0\, \mathrm{d}\Omega \mathrm{d}V = \Omega \int f_0\, \mathrm{d}V, \\ n\mathbf{u}\Omega = \int \mathbf{v} f_0\, \mathrm{d}\Omega \mathrm{d}V = \Omega \int \mathbf{v} f_0\, \mathrm{d}V, \\ 0.5n[\mathbf{u}\cdot\mathbf{u} + 3(kT+\psi)]\Omega = \int 0.5\mathbf{v}\cdot\mathbf{v} f_0\, \mathrm{d}\Omega\mathrm{d}V = \Omega\int 0.5\mathbf{v}\cdot\mathbf{v} f_0\,\mathrm{d}V. \end{gathered} \tag{2-4.10}$$

Since the distribution is homogeneous, and it does not involve the spatial variables, the space integration gives the total volume Ω in front of integration on velocity space. Solving Eq. 2-4.10 with Eq. 2-4.9, we can obtain the tree parameters. *Here, the main contribution of this paper is the internal mechanical energy is introduced in the energy conservation equation, based which the improved theoretical EDF derived as follows.*

Using the Gaussian integrals and doing the mathematical works as deriving MBD function [6], from Eq. 2-4.10, we obtain

$$\begin{gathered} n = \int f_0\,\mathrm{d}V = d(\pi\gamma)^{3/2}, \quad d = \frac{n}{(\pi\gamma)^{3/2}}, \\ n\mathbf{u} = \int(\mathbf{v}-\boldsymbol{\beta}) f_0\,\mathrm{d}V + \int \boldsymbol{\beta} f_0\,\mathrm{d}V = 0 + n\boldsymbol{\beta}, \qquad \boldsymbol{\beta} = \mathbf{u}, \end{gathered} \tag{2-4.11}$$

and especially the one for the energy conservation involving ψ

$$\begin{gathered} 0.5n[\mathbf{u}\cdot\mathbf{u} + 3(kT+\psi)] = \int 0.5\mathbf{v}\cdot\mathbf{v} f_0\,\mathrm{d}V = \int 0.5(\boldsymbol{v}-\boldsymbol{\beta})\cdot(\boldsymbol{v}-\boldsymbol{\beta}) f_0\,\mathrm{d}V + 0.5n\boldsymbol{v}\cdot\boldsymbol{v}, \\ 3n(kT+\psi) = \frac{n}{(\pi\gamma)^{3/2}} \times \frac{3\gamma(\pi\gamma)^{3/2}}{2} = \frac{3\gamma n}{2}, \quad \gamma = 2(kT+\psi). \end{gathered} \tag{2-4.12}$$

A substitution of the parameters obtained in Eqs. 2.4.11~12 into Eq. 2-4.9 gives the new amended EDF as

$$f_0 = \frac{n}{[2\pi(kT+\psi)]^{3/2}} \exp\left[-\frac{(\boldsymbol{v}-\boldsymbol{u})\cdot(\boldsymbol{v}-\boldsymbol{u})}{2(kT+\psi)}\right]. \tag{2-4.13}$$

Using this amended EDF and the tensor notations [113-115], we have the following integration formulations

$$\begin{gathered} \int f_0\,\mathrm{d}V = n, \qquad \int f_0\,(v_i - u_i)\mathrm{d}V = 0, \\ \int f_0\,(v_i-u_i)(v_j-u_j)\mathrm{d}V = n(kT+\psi)\delta_{ij}, \qquad \int f_0\,(v_i-u_i)(v_j-u_j)(v_l-u_l)\mathrm{d}V = 0, \\ \int f_0\,(v_i-u_i)(v_j-u_j)(\boldsymbol{v}-\boldsymbol{u})\cdot(\boldsymbol{v}-\boldsymbol{u})\mathrm{d}V = 5n(kT+\psi)^2\delta_{ij}. \end{gathered} \tag{2-4.14}$$

Using the notation $kT + \psi = \bar{T}$ for the mechanical energy included, it is not difficult to demonstrate that

$$\begin{gathered} \int f_0 = n, \qquad \int f_0\, v_i = nu_i, \qquad \int f_0\, v_i v_j = n\bar{T}\delta_{ij} + nu_iu_j, \\ \int f_0\, v_iv_jv_l = n\bar{T}(u_l\delta_{ij} + u_i\delta_{lj} + u_j\delta_{il}) + nu_iu_ju_l, \\ \int f_0\, v_iv_jv_lv_l = 5n\bar{T}^2\delta_{ij} + n\bar{T}(7u_iu_j + u_lu_l\delta_{ij}) + nu_iu_ju_lu_l. \end{gathered} \tag{2-4.15}$$

3. Conservation laws

Here, we examine if the developed amended EDF satisfying BTE, can be used to obtain the macroscopic conservation laws, which has not been fully addressed by using MBD function. If the answer is positive, this amended EDF will provide the basis to construct an improved LBM scheme to simulate various complex physical problems dominated by the changes of internal energy. This is because the general concepts in BTE are not only applicable for dilute gases, but also for much denser fluids.

3.1 Conservation theorem in a differential form

The EDF $f(\boldsymbol{x},\boldsymbol{v},t)$ satisfies a partial differential equation

$$\left(\frac{\partial}{\partial t}+\boldsymbol{v}\cdot\frac{\partial}{\partial \mathbf{x}}+\widehat{\boldsymbol{F}}_v\cdot\frac{\partial}{\partial \boldsymbol{v}}+\hat{\vartheta}_K\frac{\partial}{\partial(0.5\boldsymbol{v}\cdot\boldsymbol{v})}\right)f=\left(\frac{\partial f}{\partial t}\right)_C,\qquad \widehat{\boldsymbol{F}}_v=\frac{\mathrm{d}\boldsymbol{v}}{\mathrm{d}t},\qquad \hat{\vartheta}_K=\frac{\mathrm{d}}{\mathrm{d}t}\left(\frac{\boldsymbol{v}\cdot\boldsymbol{v}}{2}\right)=\frac{\mathrm{d}\widehat{K}}{\mathrm{d}t}. \tag{3-1.1}$$

Here, a new term on the change of kinetic energy energy $\frac{\boldsymbol{v}\cdot\boldsymbol{v}}{2}=\widehat{K}$ introduced, since the amendes EDF includes the internal energy as marcroscopic parameter, and its change effect needs to be explored that is a new contribution of the paper.

The instant time change rate of the streaming velocity gives the *instant* acceleration per unit particle, i.e. the *instant* force $\widehat{\boldsymbol{F}}_v$ per unit partice, while the time change rate of the kinetic energy per unit partice gives the insatnt energy change rate $\hat{\vartheta}_K$. Obvously, The instnat values of the force $\widehat{\boldsymbol{F}}_v$ and the energy change rate $\hat{\vartheta}_K$involve not only the internal motion variables, such as instant stress and streaming velcocity, but also the external quantities, such as the body force and the external energy source per unit mass. However, in the equilibirum state, the internal contributions to them are canceled each other according to the Newton's second law, so that in the averaged equilibrium state governed by BTE, the following external force $\widehat{\boldsymbol{F}}$ and external energy gereration rate $\hat{\vartheta}$ are the averaged ones

$$\langle n\hat{\vartheta}_\varepsilon\rangle=n\hat{\vartheta},\qquad \langle n\widehat{\boldsymbol{F}}_v\rangle=n\widehat{\boldsymbol{F}}\,, \tag{3-1.2}$$

respectively represnting the external body force and the external energy gneration rate per unit particle, which are assumed being independent of the streaming process, but the macroscopic quantities, possible functions of the time, space position and macroscopic velocity prescribed by the problems.

The right-hand side of Eq. 3-1.1 represents the un-balance part caused by collision in the system. We consider a conserved property $\phi(\boldsymbol{x},\boldsymbol{v})$ with its finite value at any point of space, so that it is independent of time *t*. Multiplying Eq. 3-1.1 by this property, and then integrating the resultant equation over the phase space, we obtain

$$\begin{aligned}\int_\Omega\left[\int_V \phi(\boldsymbol{x},\boldsymbol{v})\left(\frac{\partial}{\partial t}+\boldsymbol{v}\cdot\frac{\partial}{\partial x}+\widehat{\boldsymbol{F}}_v\cdot\frac{\partial}{\partial \boldsymbol{v}}+\hat{\vartheta}_K\frac{\partial}{\partial(0.5\boldsymbol{v}\cdot\boldsymbol{v})}\right)f\mathrm{d}V\right]\mathrm{d}\Omega \\ =\int_\Omega\left[\int_V \phi(\boldsymbol{x},\boldsymbol{v})\left(\frac{\partial f}{\partial t}\right)_C\mathrm{d}V\right]\mathrm{d}\Omega,\end{aligned} \tag{3-1.3}$$

of which, the total collision term on the right-hand side vanishes, since the total system in the space is momentum conservative, although the collision term $(\partial f/\partial t)_C$ at a local point in the space is not zero. Eq. 3-1.3 is re-written as

$$\begin{aligned}\int_\Omega\Bigg\{\int_V\Bigg[&\frac{\partial(f\phi)}{\partial t}+\frac{\partial(v_i f\phi)}{\partial x_i}-f\frac{\partial(v_i\phi)}{\partial x_i}+\frac{\partial(\hat{F}_{iv}f\phi)}{\partial v_i}-\hat{F}_{iv}f\frac{\partial(\phi)}{\partial v_i}-f\phi\frac{\partial(\hat{F}_{iv})}{\partial v_i} \\ &+\frac{\partial(\hat{\vartheta}_K f\phi)}{\partial(0.5v_iv_i)}-\hat{\vartheta}_K f\frac{\partial(\phi)}{\partial(0.5v_iv_i)}-f\phi\frac{\partial(\hat{\vartheta}_K)}{\partial(0.5v_iv_i)}\Bigg]\mathrm{d}V\Bigg\}\mathrm{d}\Omega=0.\end{aligned} \tag{3-1.4}$$

Using the Green theorem in the velocity space [113-115], we can transform the volume integration in the infinite velocity space V into a surface integration on its boundary S of unit normal vector v_i at infinity, i.e.

$$\int_V \frac{\partial(\hat{F}_{iv}f\phi)}{\partial v_i}\mathrm{d}V=\int_S \hat{F}_{iv}f\phi v_i\,\mathrm{d}S=0, \tag{3-1.5}$$

since the EDF $f\to 0$, when $v_i\to\infty$ on the infinte boundary S. Furthermore, the integration on the infinite volume V, $\int_V \mathrm{d}V\frac{\partial(\hat{\vartheta}_K f\phi)}{\partial(0.5v_iv_i)}=0$, can be demonstrated as follows. Referring Fig. 2, on the shpere surface of radius r the kinetic energy is a constant $\widehat{K}=0.5v_iv_i$, so that along an arbitrary radial direction r, the differential element $d\widehat{K}=d(0.5v_iv_i)$, implying the $\widehat{K}$ is taken as a cordinate to denote the corresponding sphere. As a special case $d\widehat{K}=d(0.5v_1^2)=d\widehat{K}_1$, if the direction r is chosen as the direction of velocity cordinate v_1 in the vellocity space. Therefore, we can use the Green theorem and the property of EDF vanishing at infinite to calculate the integration

$$\int_V \mathrm{d}V\frac{\partial(\hat{\vartheta}_K f\phi)}{\partial(0.5v_iv_i)}=\int_V \frac{\partial(\hat{\vartheta}_K f\phi)}{\partial\widehat{K}}\mathrm{d}V=\int_V \frac{\partial(\hat{\vartheta}_K f\phi)}{\partial\widehat{K}_1}\mathrm{d}V=\int_S \hat{\vartheta}_K f\phi v_1\mathrm{d}S=0. \tag{3-1.6}$$

Defining the average value of variable $A(\boldsymbol{x},\boldsymbol{v},t)$ as

$$\langle A\rangle = \bar{A} = \int fA\mathrm{d}V / \int f\mathrm{d}V = \int fA\mathrm{d}V/n, \tag{3-1.7}$$

from which, when substituted into Eq. 3-1.4, and considering Eqs. 3-1.5 and 3-1.6, it follows

$$\int_\Omega \left\{\left[\frac{\partial\langle n\phi\rangle}{\partial t} + \frac{\partial\langle nv_i\phi\rangle}{\partial x_i} - \langle nv_i\frac{\partial(\phi)}{\partial x_i}\rangle - \langle n\hat{F}_{iv}\frac{\partial(\phi)}{\partial v_i}\rangle - \langle n\phi\frac{\partial(\hat{F}_{iv})}{\partial v_i}\rangle - \langle n\hat{\vartheta}_K\frac{\partial(\phi)}{\partial(0.5v_iv_i)}\rangle - \langle n\phi\frac{\partial(\hat{\vartheta}_K)}{\partial(0.5v_iv_i)}\rangle\right]\right\}\mathrm{d}\Omega = 0. \tag{3-1.8}$$

where we have completed the integration in the momentum space and noticed that $n\langle A\rangle = \langle nA\rangle$, since n is independent of $\boldsymbol{v}$.

Equation 3-1.8 is the general conservation theorem in an integration form, in which there is no restrictions on the size Ω. When we choose a small deferential volume Ω, we obtain the conservation theorem in the differential form

$$\frac{\partial\langle n\phi\rangle}{\partial t} + \frac{\partial\langle nv_i\phi\rangle}{\partial x_i} - \langle nv_i\frac{\partial(\phi)}{\partial x_i}\rangle - \langle n\hat{F}_{iv}\frac{\partial(\phi)}{\partial v_i}\rangle - \langle n\phi\frac{\partial(\hat{F}_{iv})}{\partial v_i}\rangle - \langle n\vartheta_K\frac{\partial(\phi)}{\partial(0.5v_iv_i)}\rangle - \langle n\phi\frac{\partial(\hat{\vartheta}_K)}{\partial(0.5v_iv_i)}\rangle = 0, \tag{3-1.9}$$

and furthermore

$$\frac{\partial\langle n\phi\rangle}{\partial t} + \frac{\partial\langle nv_i\phi\rangle}{\partial x_i} - \langle nv_i\frac{\partial(\phi)}{\partial x_i}\rangle - \langle n\hat{F}_{iv}\frac{\partial(\phi)}{\partial v_i}\rangle - \langle n\hat{\vartheta}_K\frac{\partial(\phi)}{\partial(0.5v_iv_i)}\rangle = 0, \tag{3-1.10}$$

since in the equilibrium state the external force $\hat{\boldsymbol{F}}_v$ and the external energy generation rate $\hat{\vartheta}_K$ are independent of the streaming velocity $\boldsymbol{v}$.

Figure 2

Fig. **2** Sphere surface of radius r on which the kinetic energy is constant.

3.2 Conservation laws

Taking a different property ϕ, from Eq. 3-1.10 we can obtain its corresponding conservation law as follows.

3.2.1 Mass conservation

Letting $\phi = m$, the constant particle mass, we obtain the mass conservation law

$$\frac{\partial\langle nm\rangle}{\partial t} + \frac{\partial\langle nv_im\rangle}{\partial x_i} = 0, \qquad \frac{\partial(nm)}{\partial t} + \frac{\partial(nu_im)}{\partial x_i} = 0. \tag{3-2.1}$$

where we have used the integration formulations of EDF given in Eq. 2-4.14~15. Since m is a constant, we obtain

$$\frac{\partial(n)}{\partial t} + \frac{\partial(nu_i)}{\partial x_i} = 0\,. \tag{3-2.2}$$

3.2.2 Momentum conservation

Letting $\phi = mv_j$, from Eq. 3-1.10, we obtain

$$\frac{\partial\langle nv_j\rangle}{\partial t} + \frac{\partial\langle nv_iv_j\rangle}{\partial x_i} - \langle nv_i\frac{\partial(v_j)}{\partial x_i}\rangle - \langle n\hat{F}_{iv}\delta_{ij}\rangle - \langle n\hat{\vartheta}\frac{\partial(v_j)}{\partial(0.5v_iv_i)}\rangle = 0, \tag{3-2.3}$$

of which,

$$\langle nv_i\,\partial v_j/\partial x_i\rangle = 0, \quad \langle n\hat{\vartheta}\frac{\partial(v_j)}{\partial(0.5v_iv_i)}\rangle = \langle n\frac{d\hat{K}}{dt}\frac{\partial(v_j)}{\partial\hat{K}}\rangle = \langle n\dot{v}_j\rangle = \langle n\hat{F}_{jK}\rangle, \tag{3-2.4}$$

due to, as mentioned, the partial derivative of velocity v_i with respect to coordinate x_i vanishes. Furthermore, from Eqs. 2-4.14~15 it follows

$$\langle v_iv_j\rangle = \langle(v_i-u_i)(v_j-u_j)\rangle + \langle v_j\rangle u_i + \langle v_i\rangle u_j - u_iu_j = p_{ij} + u_iu_j, \tag{3-2.5}$$
$$p_{ij} = \langle(v_i-u_i)(v_j-u_j)\rangle = (kT+\psi)\delta_{ij},$$

which with Eqs. 3-2.4 are substituted into Eq. 3-2.3 and using the related integration formulations, we obtain

$$\frac{\partial(nu_j)}{\partial t} + \frac{\partial(nu_iu_j)}{\partial x_i} + \frac{\partial(nkT)}{\partial x_j} + \frac{\partial(n\psi)}{\partial x_j} - n\hat{F}_j = 0, \tag{3-2.6}$$

where we have used Eq. 3-1.2 to obtain $\langle n\hat{F}_{jK}\rangle + \langle n\hat{F}_{iv}\delta_{ij}\rangle = \langle n\hat{F}_{jT}\rangle = n\hat{F}_j$.

When the mass conservation Eq. 3-2.1 introduced into Eq. 3-2.6, we obtain its first two terms

$$\frac{\partial(nu_j)}{\partial t} + \frac{\partial(nu_iu_j)}{\partial x_i} = u_j\left[\frac{\partial(n)}{\partial t} + \frac{\partial(nu_i)}{\partial x_i}\right] + n\left[\frac{\partial(u_j)}{\partial t} + u_i\frac{\partial(u_j)}{\partial x_i}\right], \tag{3-2.7}$$

which gives

$$n\left(\frac{\partial u_j}{\partial t}+u_i\frac{\partial u_j}{\partial x_i}\right)=n\frac{\mathrm{D}u_j}{\mathrm{D}t}=-\frac{\partial(nkT)}{\partial x_j}-\frac{\partial(n\psi)}{\partial x_j}+n\hat{F}_j, \tag{3-2.8}$$

that is the momentum conservation law for fluids. In this equation, on the right-hand side, the first term $\partial(nkT)/\partial x_j$ denotes the contribution from thermal pressure $\hat{p}=nkT$ given in Eq. 2-1.1, the second term $\partial(n\psi)/\partial x_j$ is the contribution from the stress tensor as shown in Eq. 2-3.10, therefore we obtain

$$n\frac{\mathrm{D}u_j}{\mathrm{D}t}=-\frac{\partial\hat{p}}{\partial x_j}+\sigma_{ji,i}+n\hat{F}_j \tag{3-2.9}$$

3.2.3 Energy conservation

Mechanical energy conservation

When we do not interest in thermal effects, the term $\partial\hat{p}/\partial x_j=0$, so that we have the momentum conservation Eq. 3-2.9 for mechanical systems. Multiplying u_j on both sides of the mechanical momentum equation, we obtain

$$n\,D(0.5u_ju_j)/Dt=\sigma_{ji,i}u_j+n\hat{F}_ju_j, \tag{3-2.10}$$

that is

$$n\,D(0.5u_ju_j)/Dt=(u_j\sigma_{ji})_{,i}-\sigma_{ji}V_{ji}+n\hat{F}_ju_j=-q_{i,i}-\sigma_{ji}V_{ji}+n\hat{F}_ju_j, \tag{3-2.11}$$

from which, when Eq. 2-2.6 used for AIME of the same mass per unit volume, it yields

$$n\,D(0.5u_ju_j)/Dt+\frac{3nD\psi}{2Dt}=-q_{i,i}+n\hat{F}_ju_j. \tag{3-2.12}$$

Here q_i is the energy-flow density vector, of which the positive value implies the energy flowing from the inside to outside of the volume. Physically, Eq. 3-2.12 is the conservation law of mechanical energy, also called as the energy flow equilibrium equation and energy flow density vector included [116-118], which represents that the summation of the time change rate of kinetic and mechanic-internal energy equals a summation of the power of the body force $n\hat{F}_j$ per volume and the power flowing into the body from outside.

Total energy conservation

To derive the total energy conservation, we take $\phi=mv_jv_j/2$ in Eq. 3-1.10 and obtain

$$\frac{\partial\langle nv_jv_j\rangle}{2\partial t}+\frac{\partial\langle nv_iv_jv_j\rangle}{2\partial x_i}-\langle nv_i\frac{\partial(v_jv_j)}{2\partial x_i}\rangle-\langle n\hat{F}_{iv}\frac{\partial(v_jv_j)}{2\partial v_i}\rangle-\langle n\hat{\vartheta}_K\frac{\partial(v_jv_j)}{2\partial(0.5v_iv_i)}\rangle=0, \tag{3-2.13}$$

where due to the same reason for Eq.3-2.4, we have

$$\langle nv_i\frac{\partial(v_jv_j)}{2\partial x_i}\rangle=0,\ \langle n\hat{F}_{iv}\frac{\partial(v_jv_j)}{2\partial v_i}\rangle=\langle n\dot{v}_{iv}v_j\delta_{ij}\rangle=\langle n\frac{\mathrm{d}}{\mathrm{d}t}[(v_iv_i)_v/2]\rangle=\langle n\hat{\vartheta}_v\rangle, \tag{3-2.14}$$

from which, when substituted into Eq. 3-2.13 and using the result by Eq. 3-1.2

$$\langle n\hat{\vartheta}_v\rangle+\langle n\hat{\vartheta}_K\frac{\partial(v_jv_j)}{2\partial(0.5v_iv_i)}\rangle=\langle n\hat{\vartheta}_T\rangle=n\hat{F}_ju_j+n\hat{\vartheta}\ , \tag{3-2.15}$$

it follows

$$\frac{\partial\langle nv_jv_j\rangle}{2\partial t}+\frac{\partial\langle nv_iv_jv_j\rangle}{2\partial x_i}-n\hat{F}_ju_j-n\hat{\vartheta}\quad=0. \tag{3-2.16}$$

Using Gaussian integrations [99], we obtain

$$\langle v_jv_j\rangle=3(kT+\psi)+u_ju_j,\qquad \langle v_iv_jv_j\rangle=5(kT+\psi)u_i+u_iu_ju_j, \tag{3-2.17}$$

by which, the first two terms on the left-hand side in Eq. 3-2.16 become

$$\frac{n\mathrm{D}\left[\frac{3(kT+\psi)}{2}+\frac{u_ju_j}{2}\right]}{\mathrm{D}t}+\left[\frac{3(kT+\psi)}{2}+\frac{u_ju_j}{2}\right]\left[\frac{\partial(n)}{\partial t}+\frac{\partial(nu_i)}{\partial x_i}\right]+\frac{\partial[n(kT+\psi)u_i]}{\partial x_i}=\frac{n\mathrm{D}\left[\frac{3(kT+\psi)}{2}+\frac{u_ju_j}{2}\right]}{\mathrm{D}t}+\frac{\partial[n(kT+\psi)u_i]}{\partial x_i}, \tag{3-2.18}$$

where the mass conservation Eq. 3-2.1 has been used. Furthermore, defining

$$\frac{\partial[n(kT)u_i]}{\partial x_i} = h_{i,i}, \quad (3\text{-}2.19)$$

and considering

$$\frac{\partial[n\langle\psi\rangle u_i]}{\partial x_i} = \frac{\partial(n\psi)}{\partial x_i}u_i + n\psi\frac{\partial u_i}{\partial x_i} = -\sigma_{ij,j}u_i + n\psi\frac{\partial u_i}{\partial x_i} = q_{j,j} + \sigma_{ij}u_{i,j} + n\psi\frac{\partial u_i}{\partial x_i} = 0, \quad (3\text{-}2.20)$$

obtained from Eq. 2-3.10 and Eq. 2-3.16, we can arrange Eq. 3-2.16 as

$$\frac{n\mathrm{D}(3kT/2)}{\mathrm{D}t} + \frac{n\mathrm{D}(u_j u_j/2)}{\mathrm{D}t} + \frac{3n\mathrm{D}\psi}{2\mathrm{D}t} + h_{i,i} - n\hat{F}_j u_j - n\hat{\vartheta} \quad = 0. \quad (3\text{-}2.21)$$

When the conservation of mechanical energy in Eq. 3-2.12 is introduced into Eq. 3-2.21, and considering Eq. 2-2.6 and Eq. 2-3.13 averagely giving $q_{i,i} = \sigma_{ij}V_{ij}$, we obtain the thermal energy conservation equation

$$\frac{n\mathrm{D}[3kT/2]}{\mathrm{D}t} = -h_{i,i} + q_{i,i} + n\hat{\vartheta} \quad = -h_{i,i} + \sigma_{ij}V_{ij} + n\hat{\vartheta} \quad . \quad (3\text{-}2.22)$$

Physically, on the right-hand side of this equation, the first term denotes the thermal energy flow, the second term is the tress power, which transforms into thermal energy due to viscosity, and the third one is the energy generation from the external energy source.

It has been noted that the conservation laws derived from BTE by introducing the second order terms of partial derivatives of velocity with respect to x_i such as by [99]. Also, as reported in many references, by using the Chapman-Enskog expansions, a multi-scaling expansion [18], to express EDF and its derivatives in the forms of small parameter ϵ, the conservation laws are derived. Here, based on the amended EDF, we can directly derive the conservation laws without additional higher order derivatives of the velocities, or the Chapman-Enskog expansions. It is more important, by adding the terms of the partial derivatives of EDF with respect to the streaming velocity and the instant kinetic energy, the resultant energy conservation equation includes the external energy generation source in it, which has not found in the current publications. The introduced internal mechanical energy in EDF involves the gradient of the velocity, which was not considered in the Boltzmann's theory for dilute ideal gases. The amended theoretical EDF provides a complete theory on LBM.

4. Improved lattice Boltzmann method

The sections 2 and 3 confirm the following key points: 1) the amended EDF satisfies the Boltzmann's H theorem and the three conservation laws in continuum mechanics, so that it is the theoretical solution of BTE; 2) in EDF, there are three macroscopic parameters: mass density, mean velocity and internal energy, which respectively are functions of time and space point, therefore at different points in the time-space frame, the corresponding EDFs generally are different; 3) if we know the three macroscopic parameters at a point in the time-space frame, we will know the corresponding EDF at the same point, the solution at this point of BTE; 4) in a reverse case, if we obtain the solution of BTE at a point, we will know the corresponding EDF, so that the three macroscopic parameters of continuum mechanics can be derived from the moment equations.

The aim of LBM is to obtain the solution of BTE at every point in the time-space frame, then to obtain the macroscopic parameters which are the solution of the problems in continuum mechanics. To reach this aim, the discrete BTE is necessary. Here, based on the amended EDF, we develop an improved LBM, of which the main improvement is the total internal energy as a macroscopic parameter required to be updated in each time step.

4.1 Discrete lattice Boltzmann equation

It has been shown that discrete LBE can be obtained from the continuous BTE, see for examples, [29, 30-32]. For a single particle *I*, the BGK form of the continuous BTE [13,34,35] can be modified as

$$\left\{\frac{\partial}{\partial t} + v_i\frac{\partial}{\partial x_i} + \dot{v}_i\frac{\partial}{\partial v_i} + \hat{\vartheta}_K\frac{\partial}{\partial(0.5v\cdot v)}\right\}f_I = -\frac{1}{\tau}(f_I - f_0^I), \quad (4\text{-}1.1)$$

in which, a new term involving energy as shown in Eq. 3-1.1 is added, and the amended EDF f_0^I for 3-D case is given in Eq. 2-4.13, when using the total internal energy per unit particle $\hat{\varepsilon}$ defined in Eq. 2-4.1, it is

$$f_0^I(\rho,\hat{\varepsilon},u_i,v_i) = \frac{\rho}{(4\pi\hat{\varepsilon}/3)^{3/2}}\exp^{\frac{-3(v_i-u_i)(v_i-u_i)}{4\hat{\varepsilon}}}, \quad (4\text{-}1.2)$$

which is the function of the particle streaming velocity v_i and the three macroscopic variables: mass density ρ, mean velocity u_i and internal energy $\hat{\varepsilon}$. The energy parameter including the thermal and mechanical ones is defined as

$$\hat{\varepsilon} = 3\bar{T}/2 = \begin{cases} 3kT/2, & \text{for ideal gases and fluids,} \\ 3\psi/2\,, & \text{for non}-\text{thermal viscous fluids,} \\ 3(kT+\psi)/2, & \text{for thermal viscous fluids,} \end{cases} \tag{4-1.3}$$

which is applied to the ideal gases / fluids, the non-thermal viscous fluids, and the thermal viscous fluids, respectively. The dimension of the internal energy per unit particle / mass is $\mathrm{Nm/kg} = (\mathrm{ms}^{-1})^2$, so that the ratio of the kinetic energy over the internal energy, $0.5\boldsymbol{u}\cdot\boldsymbol{u}/\hat{\varepsilon}$, is non-dimensional parameter. For example, in the ideal gas case, we have

$$\frac{3\boldsymbol{u}\cdot\boldsymbol{u}}{2\hat{\varepsilon}} = \frac{3\rho\boldsymbol{u}\cdot\boldsymbol{u}}{3\rho kT} = \frac{\hat{p}\boldsymbol{u}\cdot\boldsymbol{u}/C^2}{\hat{p}} = M^2, \qquad M = \frac{u}{C} = \frac{u}{\sqrt{kT}}, \tag{4-1.4}$$

where we have used Eq. 2-1.1 for the definition of the gas pressure, and the relationship $\hat{p} = \rho C^2$ between the dynamic pressure $\hat{p}$ and the sound speed C for the barotropic fluid [113-115], and M is the Mach number.

Making a time integration of Eq. 4-1.1 from time t to $t+\delta t = t+1$, we obtain the change of the EDF from the original equilibrium state (x_i, v_i, t) to its state $(x_i + e_I^i, v_i, t+1)$ due the velocity change e_I^i, therefore we have

$$f_I(x_i + e_I^i, v_i, t+1) - f_I(x_i, v_i, t) = -\frac{1}{\tau_f}(f_I - f_0^I) - F_I - \widehat{\Theta}_I, \tag{4-1.5}$$

$$\tau_f = \frac{\tau}{\delta_t}, \quad \dot{v}_i \times (\delta t = 1)\frac{\partial f_I}{\partial v_i} = F_I = \hat{F}_I^i \frac{\partial f_I}{\partial v_i}, \;\; \hat{F}_I^i = \dot{v}_I, \quad \hat{\vartheta}_K \times (\delta t = 1)\frac{\partial f_I}{\partial(0.5\boldsymbol{v}\cdot\boldsymbol{v})} = \widehat{\Theta}_I. \tag{4-1.6}$$

Here, $\dot{v}_I$ denotes the particle acceleration or the particle force per unit mass, that is assumed as a constant during the small time-period δt. The velocities e_I^i at the nodes I are referred to as the *microscopic velocities*. The force F_I consists of the *particle internal interaction force* and the *possible external force* acted at the particle. If there is no external forces, the internal interaction forces between the two particles satisfy the third Newton's law, so that its summation over the total particles vanishes. Also, the term $\widehat{\Theta}_I$ is the contribution from energy generation rate $\hat{\vartheta}_K$, which vanishes if no external energy generation source in the problem.

Using Eqs. 2-4.14~15 by the summations over particle I with velocity v_{Ij} replaced by the velocities e_I^j, and $n = \rho$, as well as noting $\partial f_I/\partial(0.5\boldsymbol{v}\cdot\boldsymbol{v}) = -1.5 f_I/\hat{\varepsilon}$ and $\partial f_I/\partial v_i = -1.5 f_I(v_i - u_i)/\hat{\varepsilon} = -3 f_I(\bar{v}_i - \bar{u}_i)/\sqrt{2\hat{\varepsilon}}$, the following moment equations can be obtained,

$$\sum_I F_I = \int_V \hat{F}_i \frac{\partial f}{\partial v_i}\mathrm{d}V = 0, \tag{4-1.7}$$

$$\begin{gathered} \sum_I \widehat{\Theta}_I = \int_V \hat{\vartheta}_K \frac{\partial f_I}{\partial(0.5\boldsymbol{v}\cdot\boldsymbol{v})}\mathrm{d}V = -\int_V \frac{3\hat{\vartheta}_K f_I}{2\hat{\varepsilon}}\mathrm{d}V = -\frac{3\rho\tilde{\vartheta}}{2\hat{\varepsilon}}, \\ \sum_I F_I e_I^j = \int_V \hat{F}_i \frac{\partial f}{\partial v_i} e_I^j \mathrm{d}V = -\frac{3\rho\tilde{F}_j}{2\hat{\varepsilon}}, \\ \sum_I \widehat{\Theta}_I e_I^j = \int_V \hat{\vartheta}_K \frac{\partial f_I}{\partial(0.5\boldsymbol{v}\cdot\boldsymbol{v})} e_I^j \mathrm{d}V = -\int_V \frac{3\hat{\vartheta}_K f_I}{2\hat{\varepsilon}} e_I^j\,\mathrm{d}V = -\frac{3\rho\tilde{\vartheta}}{2\hat{\varepsilon}} u_j\,, \end{gathered} \tag{4-1.8}$$

$$\begin{gathered} \sum_I F_I e_I^j e_I^r = \int_V \hat{F}_i \frac{\partial f}{\partial v_i} e_I^j e_I^r \mathrm{d}V = -\frac{3\rho}{2\hat{\varepsilon}}(\tilde{F}_j u_r + \tilde{F}_r u_j), \\ \sum_I \widehat{\Theta}_I e_I^j e_I^r = \int_V \hat{\vartheta}_K \frac{\partial f_I}{\partial(0.5\boldsymbol{v}\cdot\boldsymbol{v})} e_I^j e_I^r \mathrm{d}V = -\frac{3\rho\tilde{\vartheta}}{2\hat{\varepsilon}}\left(\frac{2\hat{\varepsilon}}{3}\delta_{jr} + u_r u_j\right), \end{gathered} \tag{4-1.9}$$

$$\begin{gathered} \sum_I F_I e_I^j e_I^r e_I^l = \int_V \hat{F}_i \frac{\partial f}{\partial v_i} e_I^j e_I^r e_I^l \mathrm{d}V = -\frac{3\rho}{2\hat{\varepsilon}}\left[\tilde{F}_j(\bar{T}\delta_{rl} + u_r u_l) + \tilde{F}_r(\bar{T}\delta_{jl} + u_j u_l) + \tilde{F}_l(\bar{T}\delta_{rj} + u_r u_j)\right], \\ \sum_I \widehat{\Theta}_I e_I^j e_I^r e_I^l = \int_V \hat{\vartheta}_K \frac{\partial f_I}{\partial(0.5\boldsymbol{v}\cdot\boldsymbol{v})} e_I^j e_I^r e_I^l \mathrm{d}V = -\rho\tilde{\vartheta}\left[(u_j\delta_{rl} + u_r\delta_{jl} + u_l\delta_{jr}) + \frac{3}{2\hat{\varepsilon}} u_j u_l u_r\right]. \end{gathered} \tag{4-1.10}$$

It should be noticed that the force $\tilde{F}_j$ and the energy generation rate $\tilde{\vartheta}$ respectively are the external force and the external energy generation rate per unit mass of the medium, since the internal interaction ones between the two particles are governed the third Newton's law, so that the summations cancel them.

The exponential function can be represented in the power series

$$e^x = 1 + x + \frac{x^2}{2!} + \frac{x^3}{3!} + \cdots, \tag{4-1.11}$$

of which, the radius of convergence is infinite. Approximating to the second order of $u/\sqrt{2\hat{\varepsilon}}$, we have

$$e^{-\frac{3(\mathbf{v}-\mathbf{u})\cdot(\mathbf{v}-\mathbf{u})}{4\hat{\varepsilon}}} = e^{-\frac{3\mathbf{v}\cdot\mathbf{v}}{4\hat{\varepsilon}}} e^{\frac{6\mathbf{v}\cdot\mathbf{u}-3\mathbf{u}\cdot\mathbf{u}}{4\hat{\varepsilon}}} = e^{-\frac{3\mathbf{v}\cdot\mathbf{v}}{4\hat{\varepsilon}}}\left(1+\frac{3\mathbf{v}\cdot\mathbf{u}}{2\hat{\varepsilon}}+\frac{9(\mathbf{v}\cdot\mathbf{u})^2}{8\hat{\varepsilon}^2}-\frac{3\mathbf{u}\cdot\mathbf{u}}{4\hat{\varepsilon}}\right), \tag{4-1.12}$$

from which, Eq. 4-1.2 can be approximated as

$$f_0^I(\rho,\hat{\varepsilon},\bar{u}_i,\bar{\boldsymbol{v}}_I) = \frac{\bar{f}_0^I}{(\sqrt{2\hat{\varepsilon}})^3}, \bar{f}_0^I = \rho w_I\left(1+3\bar{\boldsymbol{v}}_{\boldsymbol{I}}\cdot\bar{\boldsymbol{u}}+\frac{9(\bar{\boldsymbol{v}}_I\cdot\bar{\boldsymbol{u}})^2}{2}-\frac{3\bar{\boldsymbol{u}}\cdot\bar{\boldsymbol{u}}}{2}\right), \qquad \bar{\boldsymbol{u}} = \frac{\boldsymbol{u}}{\sqrt{2\hat{\varepsilon}}}, \tag{4-1.13}$$

in which, $\bar{\boldsymbol{u}}$ denotes the non-dimensional macroscopic velocity, and $\bar{\boldsymbol{v}}_I = \boldsymbol{v}_I/\sqrt{2\hat{\varepsilon}}$ is a non-dimensional microscopic velocity at node I, and the non-dimensional weight w_I absorbs the rest coefficient. The weight can be determined by the set of velocities of the scheme based on the moment equations. It should notice that $\left(\sqrt{2\hat{\varepsilon}}\right)^{-3}$ of dimension $[\mathrm{ms}^{-1}]^{-3}$ is used for the volume element $\mathrm{d}V$of the velocity space being non-dimensional one. Therefore, we may write Eqs. 2-4.14~15 in the following forms by means of non-dimensional velocities

$$\begin{aligned}
&\text{zero order:} \quad \textstyle\sum_I \bar{f}_0^I = \rho,\\
&\text{1st order:} \quad \textstyle\sum_I \bar{f}_0^I\,(\bar{v}_I^j - \bar{u}_j) = 0,\\
&\text{2nd order:} \quad \textstyle\sum_I \bar{f}_0^I\,(\bar{v}_I^j - \bar{u}_j)(\bar{v}_I^k - \bar{u}_k) = \rho\delta_{jk}/3,\\
&\text{3rd order:} \quad \textstyle\sum_I \bar{f}_0^I\,(\bar{v}_I^j - \bar{u}_j)(\bar{v}_I^k - \bar{u}_k)(\bar{v}_I^l - \bar{u}_l) = 0,\\
&\text{4th order:} \quad \textstyle\sum_I \bar{f}_0^I\,(\bar{v}_I^j - \bar{u}_j)(\bar{v}_I^k - \bar{u}_k)(\bar{v}_I^l - \bar{u}_l)(\bar{v}_I^l - \bar{u}_l) = 5\rho\delta_{jk}/9.
\end{aligned} \tag{4-1.14}$$

and

$$\begin{aligned}
&\text{zero order:} \quad \textstyle\sum_I \bar{f}_0^I = \rho,\\
&\text{1st order:} \quad \textstyle\sum_I \bar{f}_0^I\,\bar{v}_I^i = \rho\bar{u}_i,\\
&\text{2nd order:} \quad \textstyle\sum_I \bar{f}_0^I\,\bar{v}_I^i\bar{v}_I^j = \rho(\delta_{ij}/3 + \bar{u}_i\bar{u}_j),\\
&\text{3rd order:} \quad \textstyle\sum_I \bar{f}_0^I\,\bar{v}_I^i\bar{v}_I^j\bar{v}_I^l = \rho(\bar{u}_l\delta_{ij} + \bar{u}_i\delta_{lj} + \bar{u}_j\delta_{il})/3 + \rho\bar{u}_i\bar{u}_j\bar{u}_l,\\
&\text{4th order:} \quad \textstyle\sum_I \bar{v}_I^i\bar{v}_I^j\bar{v}_I^l\bar{v}_I^l = \frac{5\rho\delta_{ij}}{9} + \frac{\rho(7\bar{u}_i\bar{u}_j + \bar{u}_l\bar{u}_l\delta_{ij})}{3} + \rho\bar{u}_i\bar{u}_j\bar{u}_l\bar{u}_l.
\end{aligned} \tag{4-1.15}$$

It may be necessary to mention that according to the tensor rule [113-115], we have

$$\delta_{ii} = \begin{cases} 1, & \text{1-D case,}\\ 2, & \text{2-D case,}\\ 3, & \text{3-D case,} \end{cases} \tag{4-1.16}$$

so that from Eq. 2-4.15, the energy conservation equations are

$$\textstyle\sum_I \bar{f}_0^I\, v_I^i v_I^i = \begin{cases} \rho(2\hat{\varepsilon}/3 + u_iu_i), & 1-\text{D case,}\\ \rho(4\hat{\varepsilon}/3 + u_iu_i), & 2-\text{D case,}\\ \rho(6\hat{\varepsilon}/3 + u_iu_i), & 3-\text{D case.} \end{cases} \quad \textstyle\sum_I \bar{f}_0^I\, \bar{v}_I^i\bar{v}_I^i = \begin{cases} \rho(1/3 + \bar{u}_i\bar{u}_i), & 1-\text{D case,}\\ \rho(2/3 + \bar{u}_i\bar{u}_i), & 2-\text{D case,}\\ \rho(3/3 + \bar{u}_i\bar{u}_i), & 3-\text{D case.} \end{cases} \tag{4-1.17}$$

In the history, the approximated form of the original EDF with the DnQb models was developed by Qian and his colleagues [25,26,63]. Here, the number n =1,2,3 denotes the dimension of problem, while b indicates the node number of the scheme. To obtain the weights w_I, He & Luo [30] used a third Hermite formula to approximate the integrals of the moment equation, and Abe [29] assumed $w_I$having a simple truncated functional form based on $\boldsymbol{e}_I$. More generally, the Gaussian quadrature can be adopted to determine the weights for the exact values of the moment integrals [88], which is supported by the fundamental theorem [89].

It should be noticed that the moment equations in Eqs. 4-1.14~15 do not include the force effect given in Eq. 4-1.5. If there are no external forces, these moment equations are valid, but if there exist some external forces, the force effect in Eq. 4-1.5 must be included.

Figure 3

a) b)

Fig. 3 a) D2Q9 scheme for 2-D problems, b) D3Q19 scheme for 3-D problems.[100]

4.2 Schemes of LBM

Using the approximate EDF in Eq. 4-1.13, i.e.

$$\bar{f}_0^I = \rho w_I\left(1 + 3\bar{\boldsymbol{v}}_{\boldsymbol{I}}\cdot\bar{\boldsymbol{u}} + \frac{9(\bar{\boldsymbol{v}}_{\boldsymbol{I}}\cdot\bar{\boldsymbol{u}})^2}{2} - \frac{3\bar{\boldsymbol{u}}\cdot\bar{\boldsymbol{u}}}{2}\right), \tag{4-2.1}$$

the following schemes of LBM can be established in the DnQb forms.

4.2.1 1-D scheme D1Q3

For D1Q3, we choose three nodes $(-1,0,1)$ with the corresponding velocity $(-c, 0, c)$, so that from Eq. 4-2.1, it follows

$$\begin{aligned} f_0^{-1} &= \rho w_{-1}\left(1 + \frac{-3cu}{c^2} + \frac{9(cu)^2}{2c^4} - \frac{3u^2}{2c^2}\right), \quad c = \sqrt{2\hat{\varepsilon}}, \\ f_0^{0} &= \rho w_0\left(1 - \frac{3u^2}{2c^2}\right), \\ f_0^{1} &= \rho w_1\left(1 + \frac{3cu}{c^2} + \frac{9(cu)^2}{2c^4} - \frac{3u^2}{2c^2}\right). \end{aligned} \tag{4-2.2}$$

Considering the symmetry of node locations, we have no reason more favor one of them, so that to choose the same weights at the two side nodes, $w_1 = w_{-1}$, then from the first two moment equations in Eq. 2-4.15, we obtain the weights $w_1 = w_{-1} = 1/6$ and $w_0 = 4/6$.

4.2.2 2-D scheme D2Q9

For 2-D problem, we choose 9 nodes scheme shown by Fig. 3a), with the velocities and the weights at the nodes have been given in many publications, such as: [25,26,29, 30, 63,88,99], which are

$$\begin{gathered} \mathrm{v}_0 = 0, \quad w_0 = 4/9 \\ \mathrm{v}_I = \left(\cos\tfrac{I-1}{2}\pi,\ \sin\tfrac{I-1}{2}\pi\right)c, \quad w_I = 1/9, \quad (I = 1\sim 4), \\ \mathrm{v}_I = \sqrt{2}\left(\cos\tfrac{2I-9}{2}\pi, \sin\tfrac{2I-9}{2}\pi\right)c, \quad w_I = 1/36, \quad (I = 5\sim 8). \end{gathered} \tag{4-2.3}$$

4.2.3 3-D schemes D3Q19

For 3-D problems, D3Q19 scheme chooses the 19 nodes as shown by Fig. 3b). The velocities and the weights at the nodes have been presented in the wide publications, which are

$$\begin{gathered} \mathrm{v}_0 = 0, \quad w_0 = 1/3, \\ \mathrm{v}_I = \left(\cos\tfrac{I-1}{2}\pi,\ \sin\tfrac{I-1}{2}\pi,\ 0\right)c, \quad w_I = 1/18, \quad (I = 1\sim 4), \\ \mathrm{v}_I = (0,\ 0,\ \cos(I-5)\,\pi\,)c, \quad w_I = 1/18, \quad (I = 5{,}6), \\ \mathrm{v}_I = \sqrt{2}\left(\cos\tfrac{2I-13}{2}\pi, \sin\tfrac{2I-13}{2}\pi, 0\right)c, \quad w_I = 1/36, \quad (I = 7\sim 10), \\ \mathrm{v}_I = \sqrt{2}\left(\cos\tfrac{2I-21}{2}\pi, 0, \sin\tfrac{2I-21}{2}\pi\right)c, \quad w_I = 1/36, \quad (I = 11\sim 14), \\ \mathrm{v}_I = \sqrt{2}\left(0, \cos\tfrac{2I-29}{2}\pi, \sin\tfrac{2I-29}{2}\pi\right)c, \quad w_I = 1/36, \quad (I = 15\sim 18). \end{gathered} \tag{4-2.4}$$

4.3 Generalised forces

In the publications, some force models have been proposed. For example, reference [48] suggested an acceleration model to denote a fore

$$F_I = -\left(1 - \frac{1}{2\tau}\right)\frac{(\boldsymbol{v}_I - \boldsymbol{u})\cdot\boldsymbol{a}}{C_S^2} f_0, \tag{4-3.1}$$

where $\boldsymbol{a}$ denotes the macroscopic acceleration of the particle, while reference [49] proposed a physical force model to distribute the physical force on the cell particles using distribution function in the form

$$F_I = w_I\left(\frac{\boldsymbol{v}_I}{C_S^2} + \frac{(\boldsymbol{v}_I\cdot\boldsymbol{u})\boldsymbol{v}_I}{C_S^4} - \frac{\boldsymbol{u}}{C_S^2}\right)\cdot\boldsymbol{F}, \tag{4-3.2}$$

where $\boldsymbol{F}$ is the physical force vector defined by

$$\boldsymbol{F} = \nabla\rho C_S^2 - \rho\nabla(\mu_0 - \kappa\nabla^2\rho). \tag{4-3.3}$$

Here μ_0 is the chemical potential of the bulk energy of fluid, and κ denotes a gradient parameter relating the interface thickness of two-phase fluids.

In this developed method of the paper, the introduced terms of external force and energy generation resources are in Eqs 4-1.5~6 and the corresponding moment equations by Eqs. 4-1.7~10. Therefore, there is no need to use any above force models proposed in the literatures. Based on the moment Eqs. 4-1.7~10 and using non-dimensional streaming velocities $\bar{\boldsymbol{v}}_I = \frac{\boldsymbol{v}_I}{\sqrt{2\hat{\varepsilon}}}$ and $\bar{\boldsymbol{u}}_I = \frac{\boldsymbol{u}_I}{\sqrt{2\hat{\varepsilon}}}$, we define the following three generalised forces contributed by the external force and energy generation source for the three conservation equations used in subsection 4.4. They are

$$\text{mass:} \quad \bar{F}^{\mathrm{m}} = \sum_I F_I + \sum_I \hat{\Theta}_I = -\frac{3\rho\tilde{\vartheta}}{2\hat{\varepsilon}} = -3\rho\bar{\vartheta}\ , \tag{4-3.4}$$

$$\text{momentum:} \quad \bar{F}_j^{\mathrm{v}} = \sum_I F_I \bar{v}_I^j + \sum_I \hat{\Theta}_I\, \bar{v}_I^j = -\frac{3\rho\tilde{F}_j}{\sqrt{2\hat{\varepsilon}}} - \frac{3\rho\tilde{\vartheta}}{2\hat{\varepsilon}}\bar{u}_j = -3\rho(\bar{F}_j + \bar{\vartheta}\bar{u}_j), \tag{4-3.5}$$

$$\text{energy:} \quad \bar{F}_{jr}^{\mathrm{e}} = \sum_I F_I \bar{v}_I^j \bar{v}_I^r + \sum_I \hat{\Theta}_I\, \bar{v}_I^j \bar{v}_I^r = -3\rho\left[\left(\bar{F}_j\bar{u}_r + \bar{F}_r\bar{u}_j\right) - \bar{\vartheta}\left(\frac{\delta_{jr}}{3} + \bar{u}_r\bar{u}_j\right)\right], \tag{4-3.6}$$

where $\bar{F}_j = \frac{\tilde{F}_j}{\sqrt{2\hat{\varepsilon}}}$ and $\bar{\vartheta} = \frac{\tilde{\vartheta}}{2\hat{\varepsilon}}$ respectively denote the non-dimensional external force and energy generation source intensity per unit mass of the material. For the force and energy generation source at a time or space point, they can be denoted using Delta function, for example, a force applied at point $\boldsymbol{x}_a$ and at time t_b can be denoted as

$$\bar{F}_j = \frac{\tilde{F}_j\delta(x - x_a, t - t_b)}{\sqrt{2\hat{\varepsilon}}}. \tag{4-3.7}$$

4.4 Implementation

For programing, LBM equation with its characteristic time τ concerning viscosity ν of the fluid to be chosen by the problems, can be generally written as

$$\bar{f}_I\left(x_i + v_I^i, t+1\right) - \bar{f}_I(x_i, t) = -\frac{1}{\tau}\left(\bar{f}_I - \bar{f}_0^I\right) - F_I - \hat{\Theta}_I, \tag{4-4.1}$$

where F_I and $\hat{\Theta}_I$ denote the force and energy change rate, including the internal and external ones, per unit mass at point *I.* For example, the kinematic viscosity has been used in the literatures by

$$\nu = \frac{2\tau - 1}{6}\frac{(\Delta x)^2}{\Delta t} = \frac{2\tau - 1}{6}C^2\Delta t. \tag{4-4.2}$$

In the implementation processes published in most literatures, the collision step is before the streaming one. It has been noticed that in some publications, such as [41], the streaming step is arranged before the collision step, which are: a) streaming move $\boldsymbol{x}$ to $\boldsymbol{x} + \boldsymbol{v}_I$ to obtain a distribution function $\bar{f}_I^*$, then update the macroscopic parameters and the equilibrium distribution function using the moment equations; b) replacing $\bar{f}_I$ by $\bar{f}_I^*$ in Eq. 4-4.1 to collision to obtain $\bar{f}_I(\boldsymbol{x} + \boldsymbol{v}_I, t+1)$. Here we describe this process the details as follows.

Streaming step: to obtain the distribution function by using Eq. 4-2.1, i.e.

$$\bar{f}^I = \rho w_I\left(1 + 3\bar{\boldsymbol{v}}_I \cdot \bar{\boldsymbol{u}} + \frac{9(\bar{\mathbf{v}}_I\cdot\bar{\mathbf{u}})^2}{2} - \frac{3\bar{\boldsymbol{u}}\cdot\bar{\boldsymbol{u}}}{2}\right),\ \bar{\boldsymbol{u}} = \frac{\boldsymbol{u}}{\sqrt{2\hat{\varepsilon}}}\ , \bar{\boldsymbol{v}}_I = \frac{\boldsymbol{v}_I}{\sqrt{2\hat{\varepsilon}}},$$
$$\bar{f}_I(\boldsymbol{x} + \boldsymbol{v}_I, t) = \bar{f}_I^{(*)}. \tag{4-4.3}$$

Macroscopic variables update calculations: based on $\bar{f}_I^{(*)}$ and the following conservation laws with no external force included,

$$\begin{aligned}
&\text{Mass density} && \textstyle\sum_I \bar{f}_I^{(*)} = \rho^{(*)},\\
&\text{Velocity} && \textstyle\sum_I \bar{f}_I^{(*)}\, \bar{v}_I^i = (\rho\bar{u}_i)^{(*)},\\
&\text{Internal energy} && \textstyle\sum_I \bar{f}_I^{(*)}\, \bar{v}_I^i \bar{v}_I^j = (\frac{\delta_{ij}}{3}\rho + \rho\bar{u}_i\bar{u}_j)^{(*)},\\
& && \textstyle\sum_I \bar{f}_I^{(*)}\, \bar{v}_I^i \bar{v}_I^i = (\frac{\tilde{d}}{3}\rho + \rho\bar{u}_i\bar{u}_i)^{(*)},\ \ \tilde{d} = 1,2,3,\ \text{dimension number.}
\end{aligned} \tag{4-4.4}$$

Equilibrium distribution functions based on macroscopic variables (*)

$$\bar{f}_0^I(\boldsymbol{x} + \boldsymbol{v}_I, t) = \quad \bar{f}_0^{I(*)}\ . \tag{4-4.5}$$

Collision step: to obtain the distribution function

$$\bar{f}_I(\boldsymbol{x} + \boldsymbol{v}_I, t+1) = \bar{f}_I^{(*)} + \frac{1}{\tau}\left[\bar{f}_0^{I(*)} - \bar{f}_I^{(*)}\right] = \bar{f}_I^{(\vartheta+1)}. \tag{4-4.6}$$

Final macroscopic variables calculations: based on the distribution function $\bar{f}_I^{(\vartheta+1)}$ and the conservation laws including the generalised external force effect given in Eqs 4-3.4~6, i.e.

Mass: $\sum_I \bar{f}_I^{(\vartheta+1)} = \rho^{(\vartheta+1)} - \bar{F}^{\mathrm{m}(\vartheta)}$,

Velocity: $\sum_I \bar{f}_I^{(\vartheta+1)}\, \bar{v}_I^i = (\rho\bar{u}_i)^{(\vartheta+1)} - \bar{F}_i^{\mathrm{v}(\vartheta)}$ (4-4.7)

Internal energy:

$$\sum_I \bar{f}_I^{(\vartheta+1)}\, \bar{v}_I^i \bar{v}_I^j = (\tfrac{\delta_{ij}}{3}\rho + \rho\bar{u}_i\bar{u}_j)^{(\vartheta+1)} - \bar{F}_{ij}^{\mathrm{e}(\vartheta)},$$
$$\sum_I \bar{f}_I^{(\vartheta+1)}\, \bar{v}_I^i \bar{v}_I^i = (\tfrac{\tilde{d}}{3}\rho + \rho\bar{u}_i\bar{u}_i)^{(\vartheta+1)} - \bar{F}_{ii}^{\mathrm{e}(\vartheta)}.$$

Here the values at the original position $(\boldsymbol{x}, t)$ marked by (ϑ), since generalised forces in Eq. 4-3.4~5 are the ones at (ϑ), which involves the physical macroscopic quantities only.

4.5 Matrix equations for implementation process

4.5.1. Implementation steps in matrix form

To investigate the performance of a scheme, it is convenience to adopt the matrix notations to express the implementation processes. For a convenience of notations, we identify the quantities at the position $(\boldsymbol{x}, t)$, the middle position after streaming $(\boldsymbol{x} + \boldsymbol{v}_I, t)$ and the last position $(\boldsymbol{x} + \boldsymbol{v}_I, t+1)$ by the super-indexes (ϑ), $(*)$ and $(\vartheta + 1)$, respectively. Therefore, the implementation process in matrix form is as follows.

Streaming: The distribution function vector $\bar{\boldsymbol{f}}^{(*)}$ at the space-time position $(\boldsymbol{x} + \boldsymbol{v}_I, t)$ is obtained, which is based on the macroscopic variable vector $\bar{\boldsymbol{U}}^{(\vartheta)}$ consisting of the mass density, momentum, and total internal energy $\hat{\varepsilon}$ of the fluid at the position $(\boldsymbol{x}, t)$ and through the streaming operation by means of the following streaming matrix $\boldsymbol{S}$,

$$\bar{\boldsymbol{f}}^{(*)} = \boldsymbol{S}\hat{\boldsymbol{\varepsilon}}^{(\vartheta)}\bar{\boldsymbol{U}}^{(\vartheta)}, \tag{4-5.1}$$

$$\boldsymbol{S} = \boldsymbol{w}\boldsymbol{V},\ \ \boldsymbol{V} = \begin{bmatrix} 1 & 0 & 0 & 1 \\ 1 & \bar{v}_1^i & \bar{v}_1^i\bar{v}_1^j & 1 \\ \vdots & \vdots & \vdots & \vdots \\ 1 & \bar{v}_N^i & \bar{v}_N^i\bar{v}_N^j & 1 \end{bmatrix},\ \ \bar{\boldsymbol{f}} = \begin{bmatrix} \bar{f}^0 \\ \bar{f}^1 \\ \vdots \\ \bar{f}^N \end{bmatrix},\ \ \hat{\boldsymbol{\varepsilon}}^{(\vartheta)} = \begin{bmatrix} 1 & 0 & 0 \\ 0 & 3 & 0 \\ \frac{-3\delta_{ij}}{2} & 0 & \frac{9}{2} \\ \frac{1}{2}\tilde{d} & 0 & \frac{-3}{2}\delta_{ij} \end{bmatrix},$$

$$\bar{\boldsymbol{U}}^{(\vartheta)} = \begin{bmatrix} \rho \\ \rho\bar{u}_i \\ \rho(\frac{\delta_{ij}}{3} + \bar{u}_i\bar{u}_j) \end{bmatrix},\ \ \bar{u}_i = \frac{u_i}{\sqrt{2\hat{\varepsilon}}}\ \ ,\ \ \boldsymbol{w} = \begin{bmatrix} w_0 & 0 & 0 & 0 \\ 0 & w_1 & 0 & 0 \\ 0 & 0 & \ddots & 0 \\ 0 & 0 & 0 & w_N \end{bmatrix},\ \ \tilde{d} = 1,2,3,$$

where $\tilde{d}$ denotes the dimension numbers, and the streaming velocity $\boldsymbol{v}_I$ is defined as

$$v_0^i = 0, \quad \bar{v}_I^i = \frac{v_I^i}{\sqrt{2\hat{\varepsilon}}}, \qquad (I = 1,2,\cdots,N), \tag{4-5.2}$$

from which it follows that

$$\bar{f}^{I(*)} = \boldsymbol{L}_I\hat{\boldsymbol{\varepsilon}}^{(\vartheta)}\bar{\boldsymbol{U}}^{(\vartheta)}, \qquad \boldsymbol{L}_I = w_I\begin{bmatrix} 1 & \bar{v}_I^i & \bar{v}_I^i\bar{v}_I^j & 1 \end{bmatrix}. \tag{4-5.3}$$

Updated calculations: The macroscopic displacement vector $\bar{\mathbf{U}}^{(*)}$ and internal energy $\hat{\varepsilon}^{(*)}$ at position $(\boldsymbol{x} + \boldsymbol{v}_I, t)$ is calculated, which is based on the obtained distribution function vector $\bar{\boldsymbol{f}}^{(*)}$ and through a conservation transformation by means of the following conservation matrix $\widetilde{\boldsymbol{V}}$,

$$\widetilde{\boldsymbol{V}}\bar{\boldsymbol{f}}^{(*)} = \bar{\boldsymbol{U}}^{(*)}, \qquad \widetilde{\boldsymbol{V}} = \begin{bmatrix} 1 & 1 & \cdots & 1 \\ 0 & \bar{v}_1^i & \cdots & \bar{v}_N^i \\ 0 & \bar{v}_1^i\bar{v}_1^j & \cdots & \bar{v}_N^i\bar{v}_N^j \end{bmatrix}. \tag{4-5.4}$$

The row equations of the matrix Eq. 4-5.4 can be respectively written as

$$\sum_{I=0}^N \bar{f}^{I(*)} = \rho^{(*)}, \qquad \sum_{I=0}^N \frac{v_I^i}{\sqrt{2\hat{\varepsilon}^{(*)}}}\bar{f}^{I(*)} = (\rho\bar{u}_i)^{(*)}, \qquad \sum_{I=0}^N \frac{v_I^i v_I^j}{2\hat{\varepsilon}^{(*)}}\bar{f}^{I(*)} = (\rho\bar{u}_i\bar{u}_j)^{(*)} + \frac{\delta_{ij}}{3}\rho^{(*)}, \tag{4-5.5}$$

which, when Eqs. 4-5.1~3 substituted, respectively yields the following conservation laws of mass, momentum, and energy,

$$\rho^{(*)} = \boldsymbol{L}_\rho\hat{\boldsymbol{\varepsilon}}^{(\vartheta)}\bar{\boldsymbol{U}}^{(\vartheta)}, \qquad \boldsymbol{L}_\rho = \sum_{\boldsymbol{I}=\boldsymbol{0}}^{\boldsymbol{N}} \boldsymbol{L}_I, \tag{4-5.6}$$
$$(\rho\bar{u}_i)^{(*)} = \frac{1}{\sqrt{2\hat{\varepsilon}^{(*)}}}\boldsymbol{L}_p\hat{\boldsymbol{\varepsilon}}^{(\vartheta)}\bar{\boldsymbol{U}}^{(\vartheta)}, \qquad \boldsymbol{L}_p = \sum_{\boldsymbol{I}=\boldsymbol{0}}^{\boldsymbol{N}} v_I^i\boldsymbol{L}_I,$$
$$\frac{1}{2\hat{\varepsilon}^{(*)}}\boldsymbol{L}_e\hat{\boldsymbol{\varepsilon}}^{(\vartheta)}\bar{\boldsymbol{U}}^{(\vartheta)} = (\rho\bar{u}_i\bar{u}_i)^{(*)} + \frac{\tilde{d}}{3}\rho^{(*)}, \quad \boldsymbol{L}_e = \sum_{\boldsymbol{I}=\boldsymbol{0}}^{\boldsymbol{N}} v_I^i v_I^i\boldsymbol{L}_I.$$

From the momentum equation, we obtain

$$2\hat{\varepsilon}^{(*)}(\rho\bar{u}_i\bar{u}_i)^{(*)} = \frac{\overline{\boldsymbol{U}}^T\hat{\boldsymbol{\varepsilon}}^T\boldsymbol{L}_p^T\boldsymbol{L}_p\hat{\boldsymbol{\varepsilon}}^{(\vartheta)}\overline{\boldsymbol{U}}^{(\vartheta)}}{\rho^{(*)}}, \tag{4-5.7}$$

which, when substituted into the energy equation, gives

$$\tfrac{2}{3}\hat{\varepsilon}^{(*)}\tilde{d} = \frac{\boldsymbol{L}_e\hat{\boldsymbol{\varepsilon}}^{(\vartheta)}\overline{\boldsymbol{U}}^{(\vartheta)}}{\rho^{(*)}} - \frac{\overline{\boldsymbol{U}}^T\hat{\boldsymbol{\varepsilon}}^T\boldsymbol{L}_p^T\boldsymbol{L}_p\hat{\boldsymbol{\varepsilon}}^{(\vartheta)}\overline{\boldsymbol{U}}^{(\vartheta)}}{\rho^{(*)}\rho^{(*)}} = \frac{\overline{\boldsymbol{U}}^T\hat{\boldsymbol{\varepsilon}}^T\boldsymbol{E}\hat{\boldsymbol{\varepsilon}}^{(\vartheta)}\overline{\boldsymbol{U}}^{(\vartheta)}}{\overline{\boldsymbol{U}}^T\hat{\boldsymbol{\varepsilon}}^T\boldsymbol{H}\hat{\boldsymbol{\varepsilon}}\overline{\boldsymbol{U}}}, \qquad \boldsymbol{E} = \boldsymbol{L}_\rho^T\boldsymbol{L}_e - \boldsymbol{L}_p^T\boldsymbol{L}_p, \qquad \boldsymbol{H} = \boldsymbol{L}_\rho^T\boldsymbol{L}_\rho. \tag{4-5.8}$$

This equation provides a transformation to obtain the internal energy $\hat{\varepsilon}^{(*)}$ from the original variables before the streaming.

From the macroscopic variable vectors obtained by Eq. 4-5.4, the equilibrium distribution function $\bar{\mathbf{f}}_0^{(*)}$ can be derived by using Eq. 4-5.1 as follows

$$\bar{\boldsymbol{f}}_0^{(*)} = \boldsymbol{S}\hat{\boldsymbol{\varepsilon}}^{(*)}\widetilde{\boldsymbol{V}}\bar{\boldsymbol{f}}^{(*)}, \qquad \bar{\boldsymbol{f}}_0^{T(*)} = [\bar{f}_0^0 \quad \bar{f}_0^1 \quad \cdots \quad \bar{f}_0^N]. \tag{4-5.9}$$

Collision: From the results obtained by Eq. 4-5.1 and 4-5.9, the distribution function $\bar{\boldsymbol{f}}^{(\vartheta+1)}$ at position $(\boldsymbol{x}+\boldsymbol{v}_I, t+1)$ can be obtained by the following collision calculation

$$\bar{\boldsymbol{f}}^{(\vartheta+1)} = \left(\frac{\tau-1}{\tau}\right)\bar{\boldsymbol{f}}^{(*)} + \frac{1}{\tau}\bar{\boldsymbol{f}}_0^{(*)}. \tag{4-5.10}$$

Further-updated macroscopic variables: Using Eq. 4-5.4 and replacing the distribution function $\bar{\boldsymbol{f}}^{(*)}$ by the $\bar{\boldsymbol{f}}^{(\vartheta+1)}$ at position $(\boldsymbol{x}+\boldsymbol{v}_I, \mathrm{t}+1)$, and including the external forces as given in Eqs. 4-3.4~6, we obtain the macroscopic variables at position $(\mathbf{x}+\mathbf{v}_I, \mathrm{t}+1)$ as

$$\widetilde{\boldsymbol{V}}\bar{\boldsymbol{f}}^{(\vartheta+1)} = \overline{\boldsymbol{U}}^{(\vartheta+1)} + \overline{\boldsymbol{F}}^{(\vartheta)}, \qquad \overline{\boldsymbol{U}}^{(\vartheta+1)} = \widetilde{\boldsymbol{V}}\bar{\boldsymbol{f}}^{(\vartheta+1)} - \overline{\boldsymbol{F}}^{(\vartheta)}, \qquad \overline{\boldsymbol{F}}^{(\vartheta)} = \begin{bmatrix}\bar{F}^{\mathrm{m}(\vartheta)} \\ \bar{F}_i^{\mathrm{v}(\vartheta)} \\ \bar{F}_{ij}^{\mathrm{e}(\vartheta)}\end{bmatrix}. \tag{4-5.11}$$

4.5.2 Integrated transformation equation

The integrated transformation equation of LBM can be derived by combining the equations of each step given in sub-section 4.5.1. Substituting Eq. 4-5.10 into Eq. 4-5.11, we obtain

$$\overline{\boldsymbol{U}}^{(\vartheta+1)} = \widetilde{\boldsymbol{V}}\left\{\left(\frac{\tau-1}{\tau}\right)\bar{\boldsymbol{f}}^{(*)} + \frac{1}{\tau}\bar{\boldsymbol{f}}_0^{(*)}\right\} - \overline{\boldsymbol{F}}^{(\vartheta)}, \tag{4-5.12}$$

from which, when Eq. 4-5.1 and Eq. 4-5.9 substituted, it follows

$$\overline{\boldsymbol{U}}^{(\vartheta+1)} = \widehat{\boldsymbol{S}}\overline{\boldsymbol{U}}^{(\vartheta)} - \overline{\boldsymbol{F}}^{(\vartheta)}, \tag{4-5.13}$$

$$\widehat{\boldsymbol{S}} = \left\{\left(\frac{\tau-1}{\tau}\right)\widehat{\boldsymbol{V}} + \frac{1}{\tau}\widehat{\boldsymbol{V}}\widehat{\boldsymbol{V}}\right\}, \qquad \widehat{\boldsymbol{V}} = \widetilde{\boldsymbol{V}}\boldsymbol{S}\hat{\boldsymbol{\varepsilon}}^{(\vartheta)}, \tag{4-5.14}$$

in which the $\hat{\varepsilon}^{(*)}$ used in Eq. 4-5.6 marked (*) can be approximated by its original values $\hat{\varepsilon}^{(\vartheta)}$, so that it is updated by

$$\tfrac{2}{3}\hat{\varepsilon}^{(\vartheta+1)}\tilde{d} = \frac{\overline{\boldsymbol{U}}^{T(\vartheta)}\overline{\boldsymbol{E}}^{(\vartheta)}\overline{\boldsymbol{U}}^{(\vartheta)}}{\overline{\boldsymbol{U}}^{T(\vartheta)}\overline{\boldsymbol{H}}^{(\vartheta)}\overline{\boldsymbol{U}}^{(\vartheta)}}, \qquad \overline{\boldsymbol{E}}^{(\vartheta)} = (\hat{\boldsymbol{\varepsilon}}^T\boldsymbol{E}\hat{\boldsymbol{\varepsilon}})^{(\vartheta)}, \ \overline{\boldsymbol{H}}^{(\vartheta)} = (\hat{\boldsymbol{\varepsilon}}^T\boldsymbol{H}\hat{\boldsymbol{\varepsilon}})^{(\vartheta)}. \tag{4-5.15}$$

After the detailed investigations on the matrices $\overline{\boldsymbol{E}}^{(\vartheta)}$ and $\overline{\boldsymbol{H}}^{(\vartheta)}$, we have found that the former has a factor $2\hat{\varepsilon}^{(\vartheta)}$, but the later does not involve $\hat{\varepsilon}^{(\vartheta)}$, therefore we can write

$$\overline{\boldsymbol{E}}^{(\vartheta)} = 2\hat{\varepsilon}^{(\vartheta)}\widetilde{\boldsymbol{E}}^{(\vartheta)}, \quad \gamma^2 = \frac{3}{\tilde{d}}\frac{\overline{\boldsymbol{U}}^{T(\vartheta)}\widetilde{\boldsymbol{E}}^{(\vartheta)}\overline{\boldsymbol{U}}^{(\vartheta)}}{\overline{\boldsymbol{U}}^{T(\vartheta)}\overline{\boldsymbol{H}}^{(\vartheta)}\overline{\boldsymbol{U}}^{(\vartheta)}}, \qquad \gamma = \sqrt{\frac{\hat{\varepsilon}^{(\vartheta+1)}}{\hat{\varepsilon}^{(\vartheta)}}}, \tag{4-5.16}$$

where γ is called as the ratio of internal energy change from the step (ϑ) to $(\vartheta+1)$.

4.6 Performance investigations

4.6.1 Characteristic matrix

The performance of the scheme is governed by the matrix $\widehat{\boldsymbol{S}}$, which is essentially determined by the matrix $\widehat{\boldsymbol{V}}$ combining the streaming matrix in Eq. 4-5.1 and the updated matrix $\widetilde{\boldsymbol{V}}$ in Eq. 4-5.4 of the scheme. Therefore, this matrix is called as the *characteristic matrix* of the scheme. Using Eqs. 4-5.1, 4-5.4 and 4-5.14, we can obtain the matrix $\widehat{\boldsymbol{V}}$ in the form,

$$\begin{aligned}\widehat{\boldsymbol{V}} = \widetilde{\boldsymbol{V}}\boldsymbol{S}\hat{\boldsymbol{\varepsilon}}^{(\vartheta)} &= \begin{bmatrix} 1 & 1 & \cdots & 1 \\ 0 & \bar{v}_1^r & \cdots & \bar{v}_N^r \\ 0 & \bar{v}_1^r\bar{v}_1^s & \cdots & \bar{v}_N^r\bar{v}_N^s \end{bmatrix} \boldsymbol{w} \begin{bmatrix} 1 & 0 & 0 & 1 \\ 1 & \bar{v}_1^i & \bar{v}_1^i\bar{v}_1^j & 1 \\ \vdots & \vdots & \vdots & \vdots \\ 1 & \bar{v}_N^i & \bar{v}_N^i\bar{v}_N^j & 1 \end{bmatrix} \begin{bmatrix} 1 & 0 & 0 \\ 0 & 3 & 0 \\ \frac{-3\delta_{ij}}{2} & 0 & \frac{9}{2} \\ \frac{1}{2}\tilde{d} & 0 & \frac{-3}{2}\delta_{ij} \end{bmatrix} \\ &= \begin{bmatrix} 1 & 1 & \cdots & 1 \\ 0 & \bar{v}_1^r & \cdots & \bar{v}_N^r \\ 0 & \bar{v}_1^r\bar{v}_1^s & \cdots & \bar{v}_N^r\bar{v}_N^s \end{bmatrix} \boldsymbol{w} \begin{bmatrix} 1+\frac{\tilde{d}}{2} & 0 & -\frac{3}{2}\delta_{ij} \\ 1+\frac{\tilde{d}}{2}-\frac{3}{2}\bar{v}_1^i\bar{v}_1^j\delta_{ij} & 3\bar{v}_1^i & \frac{9}{2}\bar{v}_1^i\bar{v}_1^j-\frac{3}{2}\delta_{ij} \\ \vdots & \vdots & \vdots \\ 1+\frac{\tilde{d}}{2}-\frac{3}{2}\bar{v}_N^i\bar{v}_N^j\delta_{ij} & 3\bar{v}_N^i & \frac{9}{2}\bar{v}_N^i\bar{v}_N^j-\frac{3}{2}\delta_{ij} \end{bmatrix} \\ &= \begin{bmatrix} \left(1+\frac{\tilde{d}}{2}\right)-\frac{3}{2}k^{ij}\delta_{ij} & 3p^i & \frac{9}{2}k^{ij}-\frac{3}{2}\delta_{ij} \\ p^r\left(1+\frac{\tilde{d}}{2}\right)-\frac{3}{2}k^{rij}\delta_{ij} & 3k^{ri} & \frac{9}{2}\bar{k}^{rij}-\frac{3}{2}p^r\delta_{ij} \\ k^{rs}\left(1+\frac{\tilde{d}}{2}\right)-\frac{3}{2}k^{rsij}\delta_{ij} & 3\bar{k}^{rsi} & \frac{9}{2}\tilde{k}^{rsij}-\frac{3}{2}k^{rs}\delta_{ij} \end{bmatrix},\end{aligned} \tag{4-6.1}$$

of which, during the matrix multiplications, we have introduced the following definitions

$$\begin{gathered}\textstyle\sum_{I=0}^N w_I = 1,\ \sum_{I=0}^N w_I\,\bar{v}_I^i = p^i,\ \sum_{I=0}^N w_I\,\bar{v}_I^i\bar{v}_I^j = k^{ij},\ \ \sum_{I=0}^N w_I\,\bar{v}_I^r\bar{v}_I^s = k^{rs}, \\ \textstyle\sum_{I=0}^N w_I\,\bar{v}_I^r\bar{v}_I^i\bar{v}_I^j = \bar{k}^{rij}, \qquad \sum_{I=0}^N w_I\,\bar{v}_I^r\bar{v}_I^s\bar{v}_I^i\bar{v}_I^j = \tilde{k}^{rsij}.\end{gathered} \tag{4-6.2}$$

As discussed before, geometrically, the weights of the schemes DnQm are center-symmetrical with the center streaming velocities $v_0^i = 0$, but the streaming velocities at non-central nodes are anti-center-symmetrical. As a result of this, we have $p^i = 0 = \bar{k}^{rij}$, so that the characteristic matrix in Eq. 4-6.1 reduces to

$$\widehat{\mathbf{V}} = \begin{bmatrix} \widehat{V}_1 & 0 & \widehat{V}_{13} \\ 0 & \widehat{V}_2 & 0 \\ \widehat{V}_{31} & 0 & \widehat{V}_3 \end{bmatrix}, \tag{4-6.3}$$

$$\widehat{V}_1 = \left(1+\tfrac{\tilde{d}}{2}\right)-\tfrac{3}{2}k^{ij}\delta_{ij},\quad \widehat{V}_2 = 3k^{ri},\quad \widehat{V}_3 = \tfrac{9}{2}\tilde{k}^{rsij}-\tfrac{3}{2}k^{rs}\delta_{ij},\quad \widehat{V}_{13} = \tfrac{9}{2}k^{ij}-\tfrac{3}{2}\delta_{ij},\quad \widehat{V}_{31} = k^{rs}\left(1+\tfrac{\tilde{d}}{2}\right)-\tfrac{3}{2}k^{rsij}\delta_{ij}.$$

For different definitions of streaming velocity, the values of above terms are given as follows.

$a)$ $v_I^i = \sqrt{2\hat{\varepsilon}}\beta_I^i,\ \beta_I^i$ denotes the unit directional vector at point *I*.

$$k^{ij} = \textstyle\sum_{I=0}^N w_I\,\beta_I^i\beta_I^j, \qquad k^{rs} = \sum_{I=0}^N w_I\,\beta_I^r\beta_I^s, \qquad k^{ri} = \sum_{I=0}^N w_I\,\beta_I^r\beta_I^i, \qquad k^{rsij} = \sum_{I=0}^N w_I\,\beta_I^r\beta_I^s\beta_I^i\beta_I^j. \tag{4-6.4}$$

b) $v_I^i = \beta_I^i$,

$$k^{ij} = \textstyle\sum_{I=0}^N w_I\frac{\beta_I^i\beta_I^j}{2\hat{\varepsilon}}, \qquad k^{rs} = \sum_{I=0}^N w_I\frac{\beta_I^r\beta_I^s}{2\hat{\varepsilon}}, \qquad k^{ri} = \sum_{I=0}^N w_I\frac{\beta_I^r\beta_I^i}{2\hat{\varepsilon}}, \qquad k^{rsij} = \sum_{I=0}^N w_I\frac{\beta_I^r\beta_I^s\beta_I^i\beta_I^j}{4\hat{\varepsilon}^2}. \tag{4-6.5}$$

It should be noted that for case a), the change of internal energy $2\hat{\varepsilon}$ is included in the matrix $\widehat{\boldsymbol{V}}$. Therefore, for the problems that involves the internal energy changes not neglected, the matrix $\widehat{\boldsymbol{V}}$ should be updated for each cell. In the case b), the internal energy is shown in the equation, and it can be directly updated, if necessary, in simulations.

4.6.2 Eigenvalues of characteristic matrix

For 3-D problems, the displacement vector defined is a 10-row vector: 1 mass density, 3 velocity components and 6 components of symmetrical tensor $u_i u_j$, so that the characteristic matrix in Eq. 4-6.3 is a 10×10 matrix, and for 1-D and 2-D problems they are respectively a 3×3 and a 6×6 matrix. Generally, the eigenvalue analysis of the matrix with higher order than 3×3 cannot be done by hand, but for the type of matrix in Eq. 4-6.3 can be analyzed as follows.

In 3-D case, the displacement vector and the characteristic matrix in Eq. 4-6.3 can be respectively written as

$$\overline{\boldsymbol{U}} = \begin{bmatrix} \rho \\ \rho u_1 \\ \rho u_2 \\ \rho u_3 \\ \rho\left(\frac{1}{3} + u_1 u_1\right) \\ \rho u_1 u_2 \\ \rho u_1 u_3 \\ \rho\left(\frac{1}{3} + u_2 u_2\right) \\ \rho u_2 u_3 \\ \rho\left(\frac{1}{3} + u_3 u_3\right) \end{bmatrix}, \quad \widehat{\boldsymbol{V}} = \begin{bmatrix} \hat{V}_1 & 0 & 0 & 0 & \hat{V}_{13}^{11} & 2\hat{V}_{13}^{12} & 2\hat{V}_{13}^{13} & \hat{V}_{13}^{22} & 2\hat{V}_{13}^{23} & \hat{V}_{13}^{33} \\ 0 & \hat{V}_2^{11} & \hat{V}_2^{12} & \hat{V}_2^{13} & 0 & 0 & 0 & 0 & 0 & 0 \\ 0 & \hat{V}_2^{21} & \hat{V}_2^{22} & \hat{V}_2^{23} & 0 & 0 & 0 & 0 & 0 & 0 \\ 0 & \hat{V}_2^{31} & \hat{V}_2^{32} & \hat{V}_2^{33} & 0 & 0 & 0 & 0 & 0 & 0 \\ \hat{V}_{31}^{11} & 0 & 0 & 0 & \hat{V}_3^{1111} & 2\hat{V}_3^{1112} & 2\hat{V}_3^{1113} & \hat{V}_3^{1122} & 2\hat{V}_3^{1123} & \hat{V}_3^{1133} \\ \hat{V}_{31}^{12} & 0 & 0 & 0 & \hat{V}_3^{1211} & 2\hat{V}_3^{1212} & 2\hat{V}_3^{1213} & \hat{V}_3^{1222} & 2\hat{V}_3^{1223} & \hat{V}_3^{1233} \\ \hat{V}_{31}^{13} & 0 & 0 & 0 & \hat{V}_3^{1311} & 2\hat{V}_3^{1312} & 2\hat{V}_3^{1313} & \hat{V}_3^{1322} & 2\hat{V}_3^{1323} & \hat{V}_3^{1333} \\ \hat{V}_{31}^{22} & 0 & 0 & 0 & \hat{V}_3^{2211} & 2\hat{V}_3^{2212} & 2\hat{V}_3^{2213} & \hat{V}_3^{2222} & 2\hat{V}_3^{2223} & \hat{V}_3^{2233} \\ \hat{V}_{31}^{23} & 0 & 0 & 0 & \hat{V}_3^{2311} & 2\hat{V}_3^{2312} & 2\hat{V}_3^{2313} & \hat{V}_3^{2322} & 2\hat{V}_3^{2323} & \hat{V}_3^{2333} \\ \hat{V}_{31}^{33} & 0 & 0 & 0 & \hat{V}_3^{3311} & 2\hat{V}_3^{3312} & 2\hat{V}_3^{3313} & \hat{V}_3^{3322} & 2\hat{V}_3^{3323} & \hat{V}_3^{3333} \end{bmatrix}. \tag{4-6.6}$$

We can write the characteristic matrix in a block form

$$\widehat{\boldsymbol{V}} = \begin{bmatrix} \boldsymbol{A}_{4\times4} & \boldsymbol{B}_{4\times6} \\ \boldsymbol{C}_{6\times4} & \boldsymbol{D}_{6\times6} \end{bmatrix}, \tag{4-6.7}$$

where each block matrix consists of the elements at the corresponding positions identified by the line and row subscripts in the matrix $\widehat{\boldsymbol{V}}$ in Eq. 4-6.6. The characteristic equation for the eigenvalues of the matrix $\widehat{\mathbf{V}}$ is given by the following equation

$$\left|\widehat{\boldsymbol{V}} - \kappa \boldsymbol{I}_{10\times10}\right| = \begin{vmatrix} \boldsymbol{A}_{4\times4} - \kappa \boldsymbol{I}_{4\times4} & \boldsymbol{B}_{4\times6} \\ \boldsymbol{C}_{6\times4} & \boldsymbol{D}_{6\times6} - \kappa \boldsymbol{I}_{6\times6} \end{vmatrix} = 0. \tag{4-6.8}$$

Using the Schur's determinant identity [121], the determinant in Eq. 4-6.8 is calculated as

$$|\boldsymbol{A}_{4\times4} - \kappa \boldsymbol{I}_{4\times4}| \neq 0, \quad \left|\widehat{\boldsymbol{V}} - \kappa \boldsymbol{I}_{10\times10}\right| = |\boldsymbol{A}_{4\times4} - \kappa \boldsymbol{I}_{4\times4}|\left|\widetilde{\boldsymbol{D}}_{6\times6}\right|, \tag{4-6.9}$$

$$\widetilde{\boldsymbol{D}}_{6\times6} = \boldsymbol{D}_{6\times6} - \kappa \boldsymbol{I}_{6\times6} - \boldsymbol{C}_{6\times4}(\boldsymbol{A}_{4\times4} - \kappa \boldsymbol{I}_{4\times4})^{-1} \boldsymbol{B}_{4\times6},$$

or

$$|\boldsymbol{D}_{6\times6} - \kappa \boldsymbol{I}_{6\times6}| \neq \boldsymbol{0}, \quad \left|\widehat{\boldsymbol{V}} - \kappa \boldsymbol{I}_{10\times10}\right| = |\boldsymbol{D}_{6\times6} - \kappa \boldsymbol{I}_{6\times6}|\left|\widetilde{\boldsymbol{A}}_{4\times4}\right|, \tag{4-6.10}$$

$$\widetilde{\boldsymbol{A}}_{4\times4} = \boldsymbol{A}_{4\times4} - \kappa \boldsymbol{I}_{4\times4} - \boldsymbol{B}_{4\times6}(\boldsymbol{D}_{6\times6} - \kappa \boldsymbol{I}_{6\times6})^{-1} \boldsymbol{C}_{6\times4}.$$

From this result, the solutions of Eq. 4-6.8 can be obtained by vanishing one of the following two lower order determinants,

$$\left|\widetilde{\mathbf{A}}_{4\times4}\right| = 0, \qquad \left|\widetilde{\mathbf{D}}_{6\times6}\right| = 0. \tag{4-6.11}$$

This analysis provides a means to derive the eigenvalues of the characteristic matrix to analyze the performance of a scheme. However, although the two determinant equations are different orders, the derived algebraic equation with same order of eigenvalue κ, so that it will not reduce the calculation tasks. It should be noted that eigenvalues of the characteristic matrix are the function of the internal energy of each simulation transformation.

4.6.3 Performance analysis based on eigenvalues of characteristic matrix

The matrix $\widehat{\boldsymbol{V}}$ is real matrix, of which the eigenvalues can be real or complex. If there exists a complex eigenvalue, its conjugate complex is also a complex eigenvalue of the matrix.

Eigenvalues and eigenvectors with their orthogonality

The eigenvalues and the corresponding eigenvectors are governed by the following eigenvalue equation

$$\widehat{\boldsymbol{V}}\boldsymbol{\Psi} = \kappa \boldsymbol{\Psi}, \qquad \left|\widehat{\boldsymbol{V}} - \kappa \boldsymbol{I}\right| = 0. \tag{4-6.12}$$

Generally, we can represent the eigenvalue equation in the matrix form

$$\widehat{\boldsymbol{V}}\boldsymbol{\Psi} = \boldsymbol{\Psi}\boldsymbol{\Lambda}, \quad \boldsymbol{\Psi} = [\boldsymbol{\psi}_1 \quad \cdots \quad \boldsymbol{\psi}_{10}], \quad \boldsymbol{\Lambda} = \mathrm{diag}(\kappa_1, \cdots, \kappa_{10}), \tag{4-6.13}$$

where κ_I and $\boldsymbol{\psi}_I$ denote the *I-th* eigenvalues and the corresponding eigenvectors. If the eigenvalues are different, the eigenvectors are independent, so that the matrix $\boldsymbol{\Psi}^{-1}$ exists. As the result of this, we have

$$\boldsymbol{\Psi}^{-1}\widehat{\boldsymbol{V}}\boldsymbol{\Psi}=\boldsymbol{\Lambda},\qquad \widehat{\boldsymbol{V}}=\boldsymbol{\Psi}\boldsymbol{\Lambda}\boldsymbol{\Psi}^{-1},\quad \widehat{\boldsymbol{V}}\widehat{\boldsymbol{V}}=\boldsymbol{\Psi}\boldsymbol{\Lambda}\boldsymbol{\Psi}^{-1}\boldsymbol{\Psi}\boldsymbol{\Lambda}\boldsymbol{\Psi}^{-1}=\boldsymbol{\Psi}\boldsymbol{\Lambda}^2\boldsymbol{\Psi}^{-1},\quad \widehat{\boldsymbol{V}}^2\boldsymbol{\Psi}=\boldsymbol{\Psi}\boldsymbol{\Lambda}^2\,, \tag{4-6.14}$$

which implies the eigenvalue of matrix $\widehat{\boldsymbol{V}}^2$ is the square of the eigenvalue of matrix $\widehat{\boldsymbol{V}}$ and the corresponding eigenvector is same as the one of matrix $\widehat{\boldsymbol{V}}$. Therefore, we have

$$\widehat{\boldsymbol{S}}=\left\{\left(\frac{\tau-1}{\tau}\right)\boldsymbol{\Psi}\boldsymbol{\Lambda}+\frac{1}{\tau}\boldsymbol{\Psi}\boldsymbol{\Lambda}^2\right\}\boldsymbol{\Psi}^{-1}. \tag{4-6.15}$$

Amplifying factor and numerical damping

The independent eigenvectors of the characteristic matrix $\widehat{\boldsymbol{V}}$ span a complete characteristic space in which the displacement vector can be expressed as

$$\overline{\boldsymbol{U}}^{(\vartheta)}=\boldsymbol{\Psi}\boldsymbol{q}^{(\vartheta)},\qquad \overline{\boldsymbol{U}}^{(\vartheta+1)}=\boldsymbol{\Psi}\boldsymbol{q}^{(\vartheta+1)}, \tag{4-6.16}$$

where $\boldsymbol{q}$ denotes a displacement vector in the characteristic space. From this expansion, when substituted into Eq. 4-5.13, it follows

$$\boldsymbol{\Psi}\boldsymbol{q}^{(\vartheta+1)}=\widehat{\boldsymbol{S}}\boldsymbol{\Psi}\boldsymbol{q}^{(\vartheta)}\,, \tag{4-6.17}$$

where the external force term has been excluded due to it is not affected the performance of the characteristic matrix. Substituting Eq. 4-6.15 into Eq. 4-6.17, we obtain

$$\boldsymbol{\Psi}\boldsymbol{q}^{(\vartheta+1)}=\left\{\left(\frac{\tau-1}{\tau}\right)\boldsymbol{\Psi}\boldsymbol{\Lambda}+\frac{1}{\tau}\boldsymbol{\Psi}\boldsymbol{\Lambda}^2\right\}\boldsymbol{q}^{(\vartheta)}\,, \tag{4-6.18}$$

which, when multiplying both side by $\boldsymbol{\Psi}^{-1}$, gives

$$\boldsymbol{q}^{(\vartheta+1)}=\left\{\left(\frac{\tau-1}{\tau}\right)\boldsymbol{\Lambda}+\frac{1}{\tau}\boldsymbol{\Lambda}^2\right\}\boldsymbol{q}^{(\vartheta)}\,. \tag{4-6.19}$$

Physically, this result implies that the performance of the scheme is determined by the eigenvalues of the characteristic matrix of the scheme.

Generally, we may assume the eigenvalues of the scheme consist of conjugate complex numbers, since the characteristic matrix is real, therefore we have

$$\boldsymbol{\Lambda}=\mathrm{diag}(\kappa_1,\kappa_1^*,\cdots), \tag{4-6.20}$$

where κ_J is complex with its conjugate one marked by *. The two complex eigenvalues can be expressed in the form

$$\kappa_J=\hat{\kappa}_J e^{-i\phi_J},\qquad \kappa_J^*=\hat{\kappa}_J e^{i\phi_J},\quad J=1,2,3,4,5. \tag{4-6.21}$$

Here $\hat{\kappa}_J$ and ϕ_J denote the module and phase angle of the complex eigenvalue, respectively. Using these notations, we can re-write Eq. 4-6.19 in the form

$$\boldsymbol{q}^{(\vartheta+1)}=\widetilde{\boldsymbol{A}}\boldsymbol{q}^{(\vartheta)}\,,\quad \widetilde{\boldsymbol{A}}=\left\{\left(\frac{\tau-1}{\tau}\right)\boldsymbol{\Lambda}+\frac{1}{\tau}\boldsymbol{\Lambda}^2\right\}. \tag{4-6.22}$$

Here $\widetilde{\boldsymbol{A}}$ is called as a complex amplifying factor matrix, which produces the amplitude amplification and the phase shift. The phase shift implies a damping effect, and the damping factor vanishes if all eigenvalues are all real. For 1-D problems, its characteristic matrix a 3×3 real matrix, so that it must have at least one real eigenvalue.

5. Examples

The key contribution of this paper is to include the internal energy parameter in the amended theoretical EDF, which allows the conservation laws to be obtained from the amended BTE. To illustrate the internal energy parameter effect, we consider the following hand-workable examples which can clearly explore the essential physical characteristics and avoid non-essential numerical treatment.

5.1. Example 1: the performance of scheme D1Q3

For this scheme, we choose three nodes $(0,-1,1)$ with the corresponding streaming velocity $(0,-v,v)$ and the weights $w_1=w_{-1}=1/6$ and $w_0=4/6$.

5.1.1 Streaming velocity $\boldsymbol{v_I^i = \sqrt{2\hat{\varepsilon}}\beta_I^i}$

Characteristic matrix and its eigenvalues

Using the method given in sub-section 4.6.1.1~2 and considering the case of no external forces, we can obtain the following matrices for this D1Q3 scheme. For this 1D problems, we have the values

$$\tilde{d} = 1,\ i = j = 1 = r = s, \tag{5-1.1}$$

from which, when substituted into Eq. 4.6.3, it follows the characteristic matrix of the system is

$$\widehat{\boldsymbol{V}} = \begin{bmatrix} \hat{V}_1 & 0 & \hat{V}_{13} \\ 0 & \hat{V}_2 & 0 \\ \hat{V}_{31} & 0 & \hat{V}_3 \end{bmatrix}, \tag{5-1.2}$$

$$\hat{V}_1 = \tfrac{3}{2} - \tfrac{3}{2}k^{11}, \quad \hat{V}_2 = 3k^{11}, \quad \hat{V}_3 = \tfrac{9}{2}\tilde{k}^{1111} - \tfrac{3}{2}k^{11}, \quad \hat{V}_{13} = \tfrac{9}{2}k^{11} - \tfrac{3}{2}, \quad \hat{V}_{31} = \tfrac{3}{2}k^{11} - \tfrac{3}{2}k^{1111}.$$

Adopting the streaming velocity form shown in Eq. 4-6.4, we obtain

$$v = \sqrt{2\hat{\varepsilon}}, \qquad \beta_0 = 0, \quad \beta_{-1} = -1, \quad \beta_1 = 1, \qquad k^{11} = 1/3 = k^{1111}, \quad \widehat{\boldsymbol{V}} = \mathbf{I}\,. \tag{5-1.3}$$

The eigenvalues and eigenvectors of the matrix $\widehat{\mathbf{V}}$ can be obtained as

$$\kappa_1 = 1,\ \boldsymbol{\psi}_1 = \begin{bmatrix}1\\0\\0\end{bmatrix};\ \kappa_2 = 1,\ \boldsymbol{\psi}_2 = \begin{bmatrix}0\\1\\0\end{bmatrix};\ \kappa_3 = 1,\ \boldsymbol{\psi}_3 = \begin{bmatrix}0\\0\\1\end{bmatrix}; \quad \boldsymbol{\Lambda} = \mathbf{I}, \quad \boldsymbol{\Psi} = \mathbf{I} = \boldsymbol{\Psi}^{-1}. \tag{5-1.4}$$

Amplifying matrix

The amplifying matrix of the transformation of the scheme in Eq. 4-6.22 is

$$\widetilde{\boldsymbol{A}} = \mathbf{I}. \tag{5-1.5}$$

Final transformation

From Eq. 4-6.12 and Eq. 4-6.16, we have the transformation

$$\overline{\boldsymbol{U}}^{(\vartheta+1)} = \overline{\boldsymbol{U}}^{(\vartheta)}, \tag{5-1.6}$$

that is

$$\begin{bmatrix} 1 & 0 & 0 \\ 0 & \frac{1}{\sqrt{2\hat{\varepsilon}}} & 0 \\ 0 & 0 & \frac{1}{2\hat{\varepsilon}} \end{bmatrix}^{(\vartheta+1)} \begin{bmatrix} \rho \\ \rho u \\ \rho(\frac{2\hat{\varepsilon}}{3} + u^2) \end{bmatrix}^{(\vartheta+1)} = \begin{bmatrix} 1 & 0 & 0 \\ 0 & \frac{1}{\sqrt{2\hat{\varepsilon}}} & 0 \\ 0 & 0 & \frac{1}{2\hat{\varepsilon}} \end{bmatrix}^{(\vartheta)} \begin{bmatrix} \rho \\ \rho u \\ \rho(\frac{2\hat{\varepsilon}}{3} + u^2) \end{bmatrix}^{(\vartheta)}, \tag{5-1.7}$$

from which, when pre-multiplying the inverse matrix of the first matrix on the left-hand side, it follows

$$\begin{bmatrix} \rho \\ \rho u \\ \rho(\frac{2\hat{\varepsilon}}{3} + u^2) \end{bmatrix}^{(\vartheta+1)} = \begin{bmatrix} 1 & 0 & 0 \\ 0 & \gamma & 0 \\ 0 & 0 & \gamma^2 \end{bmatrix}^{(\vartheta)} \begin{bmatrix} \rho \\ \rho u \\ \rho(\frac{2\hat{\varepsilon}}{3} + u^2) \end{bmatrix}^{(\vartheta)}, \qquad \gamma = \sqrt{\frac{\hat{\varepsilon}^{(\vartheta+1)}}{\hat{\varepsilon}^{(\vartheta)}}}, \tag{5-1.8}$$

where the ratio γ of internal energy change is given by Eq. 4-5.16.

5.1.2 Streaming velocity $\boldsymbol{v_I^i = \beta_I^i}$

Characteristic matrix and its eigenvalues

In this case, from Eq.4-6.5, we obtain

$$k^{11} = \frac{1}{6\hat{\varepsilon}}, \qquad k^{1111} = \frac{1}{12\hat{\varepsilon}^2}, \tag{5-1.9}$$

so that the characteristic matrix of the system is

$$\widehat{\boldsymbol{V}} = \begin{bmatrix} \hat{V}_1 & 0 & \hat{V}_{13} \\ 0 & \hat{V}_2 & 0 \\ \hat{V}_{31} & 0 & \hat{V}_3 \end{bmatrix}, \tag{5-1.10}$$

where

$$\hat{V}_1 = \frac{3}{2} - \frac{1}{4\hat{\varepsilon}}, \quad \hat{V}_2 = \frac{1}{2\hat{\varepsilon}}, \quad \hat{V}_3 = \frac{3}{8\hat{\varepsilon}^2} - \frac{1}{4\hat{\varepsilon}}, \quad \hat{V}_{13} = \frac{3}{4\hat{\varepsilon}} - \frac{3}{2}, \quad \hat{V}_{31} = \frac{1}{4\hat{\varepsilon}} - \frac{1}{8\hat{\varepsilon}^2}.$$

The characteristic equation of the system is

$$\left(\hat{V}_2 - \kappa\right)\left[\left(\hat{V}_1 - \kappa\right)\left(\hat{V}_3 - \kappa\right) - \hat{V}_{13}\hat{V}_{31}\right] = 0. \tag{5-1.11}$$

The eigenvalues of this equation are

$$\kappa_1 = \hat{V}_2,\ \boldsymbol{\psi}_1; \qquad \kappa_2 = \frac{(\hat{V}_1 + \hat{V}_3) + \sqrt{\Delta}}{2},\ \boldsymbol{\psi}_2; \qquad \kappa_3 = \frac{(\hat{V}_1 + \hat{V}_3) - \sqrt{\Delta}}{2},\ \boldsymbol{\psi}_3; \qquad \Delta = \left(\hat{V}_1 - \hat{V}_3\right)^2 + 4\hat{V}_{13}\hat{V}_{31}, \tag{5-1.12}$$

of which, κ_1 is real, and the last two ones are real if $\Delta \geq 0$, otherwise complex. Generally, as the case of complex eigenvalues, we may express these two eigenvalues as

$$\kappa_{2,3} = \hat{\kappa} e^{\pm i\phi}. \tag{5-1.13}$$

Amplifying matrix

The amplifying matrix of the transformation of this scheme in Eq. 4-6.22 is now given by

$$\widetilde{\boldsymbol{A}} = \begin{bmatrix} A_1 & 0 & 0 \\ 0 & A_2 & 0 \\ 0 & 0 & A_3 \end{bmatrix}, \quad A_I = \left\{\left(\frac{\tau - 1}{\tau}\right)\kappa_I + \frac{1}{\tau}\kappa_I^2\right\}, \quad (I = 1,2,3). \tag{5-1.14}$$

As mentioned before, in the complex eigenvalue cases, the amplifying matrices produce some damping effects causing the phase shifts in each simulation step.

5.2 1-D constant incompressible flow by D1Q3 scheme

We investigate a 1-D constant incompressible flow by the scheme D1Q3 of the weights $w_1 = w_{-1} = 1/6$, $w_0 = 4/6$ with three nodes $(0, -1, 1)$, and the corresponding streaming velocity $(0, -\sqrt{2\hat{\varepsilon}}, \sqrt{2\hat{\varepsilon}})$, of which the integrated transformation is given in subsection 5.1.1, based on which we have

$$\overline{\boldsymbol{U}}^{(\vartheta+1)} = \mathbf{I}\overline{\boldsymbol{U}}^{(\vartheta)} = \overline{\boldsymbol{U}}^{(\vartheta)}, \qquad \gamma = \sqrt{\frac{\hat{\varepsilon}^{(\vartheta+1)}}{\hat{\varepsilon}^{(\vartheta)}}} = 1. \tag{5-2.1}$$

which is the theoretical solution of the problem.

Figure 4

Fig.4 1-D stable compressed gas flow through a tube of unit cross-section area.

5.3 1-D high pressure compressible gas flow in a tube of unit cross-section area

As shown in Fig. 4, a horizontal tube of length L and unit cross-section area $\mathrm{A} = 1$ locates along $O - x$ axis. We assume that the left end of the tube connected to a very high pressed gas tank of pressure p_0 keeping a prescribed constant, and its right end at $x = \mathrm{L}$ connecting to the atmospheric pressure p_{L}, so that the difference of pressures at the two ends produces a flow in the tube. The governing equations and theoretical analysis of the problem are discussed for two cases.

5.3.1 Transient analysis before stable flow

Considering the fluid is compressible and barotropic, we respectively have its conservation equations of mass and momentum, and state equation

$$\frac{\partial \rho}{\partial t} + \frac{\partial(\rho u)}{\partial x} = \frac{\mathrm{D}\rho}{\mathrm{D}t} + \rho\frac{\partial u}{\partial x} = 0, \tag{5-3.1}$$

$$\rho\left(\frac{\partial \rho}{\partial t} + u\frac{\partial u}{\partial x}\right) = -\frac{\partial p}{\partial x}, \tag{5-3.2}$$

$$\frac{\mathrm{d}p}{\mathrm{d}\rho} = c^2: \quad p = c^2(\rho - \rho_{\mathrm{L}}) + p_L, \qquad \hat{\rho} = \rho_{\mathrm{L}} - \frac{p_L}{c^2}, \tag{5-3.3}$$

where c is a speed of sound, and $\hat{\rho}$ denotes the mass density of the gas with zero pressure. The initial and boundary conditions are

$$u(x,0)=0,\ \ p(x,0)=p_{\mathrm{L}},\ \ \rho(x,0)=\rho_{\mathrm{L}},\qquad x\in(0,\mathrm{L}), \tag{5-3.4}$$

$$p(0,t)=p_0,\quad \rho(0,t)=\rho_0,\quad p(\mathrm{L},t)=p_{\mathrm{L}},\quad \rho(\mathrm{L},t)=\rho_{\mathrm{L}}. \tag{5-3.5}$$

To find the internal energy per unit mass of the gas at a point, we define the specific volume $\varphi=1/\rho$, the volume of unit mass, and use the mass conservation Eq. 5-3.1 to obtain

$$\frac{\mathrm{d}\rho}{\rho}=-\frac{\mathrm{d}\varphi}{\varphi}=-\rho\mathrm{d}\varphi=-\frac{\partial u}{\partial x}\mathrm{d}t. \tag{5-3.6}$$

Using Eq. 2-2.3, we obtain the physical internal energy per unit mass

$$\psi(x,t)=-\int_0^t\frac{p}{\rho}\frac{\partial u}{\partial x}\mathrm{d}t=\int_{\hat{\rho}}^{\rho}\frac{p}{\rho^2}\mathrm{d}\rho=-\int_{\hat{\varphi}}^{\varphi}p\,\mathrm{d}\varphi, \tag{5-3.7}$$

$$\psi(x,0)=\int_{\hat{\rho}}^{\rho_{\mathrm{L}}}\frac{p}{\rho^2}\mathrm{d}\rho=-\int_{\hat{\varphi}}^{\varphi_{\mathrm{L}}}p\,\mathrm{d}\varphi, \tag{5-3.8}$$

and then from Eq. 4-1.3, the statistical internal energy per unit mass is

$$\hat{\varepsilon}(x,t)=\frac{3\psi(x,t)}{2},\qquad \hat{\varepsilon}(x,0)=\frac{3\psi(x,0)}{2}. \tag{5-3.9}$$

which is a function of x and *t.*

The prescribed pressures at two ends of tube produce the generalised forces at the nodes of two ends for simulation used in LBM, and from Eqs. 4-3.4~6 they are

$$\overline{\boldsymbol{F}}_0^{(\vartheta)}=\begin{bmatrix}\bar{F}_0^{\mathrm{m}(\vartheta)}\\ \bar{F}_0^{\mathrm{v}(\vartheta)}\\ \bar{F}_0^{\mathrm{e}(\vartheta)}\end{bmatrix}=\begin{bmatrix}0\\ 3\rho_0\bar{p}_0\\ 6\rho_0\bar{p}_0\bar{u}_0\end{bmatrix}^{(\vartheta)},\qquad \overline{\boldsymbol{F}}_{\mathrm{L}}^{(\vartheta)}=\begin{bmatrix}\bar{F}_{\mathrm{L}}^{\mathrm{m}(\vartheta)}\\ \bar{F}_{\mathrm{L}}^{\mathrm{v}(\vartheta)}\\ \bar{F}_{L}^{\mathrm{e}(\vartheta)}\end{bmatrix}=\begin{bmatrix}0\\ 3\rho_{\mathrm{L}}\bar{p}_{\mathrm{L}}\\ 6\rho_{\mathrm{L}}\bar{p}_{\mathrm{L}}\bar{u}_{\mathrm{L}}\end{bmatrix}^{(\vartheta)}. \tag{5-3.10}$$

Here the variable $\overline{()}$ implies its non-dimensional one by dividing with $\sqrt{2\hat{\varepsilon}_I}$ that involves step (ϑ).

5.3.2 Stable flow

When the flow reaches stable, the variables of motion are independent of the time, and Eqs 5-3.1~2 reduces to

$$\frac{\partial(\rho u)}{\partial x}=0,\qquad\qquad \rho\left(u\frac{\partial u}{\partial x}\right)=-\frac{\partial p}{\partial x}. \tag{5-3.11}$$

The integrations of Eq. 5-3.11 along the tube with respect to x yield

$$\rho(x)u(x)=\rho_0u_0=\rho_{\mathrm{L}}u_{\mathrm{L}}=\text{constant}, \tag{5-3.12}$$

$$p(x)=p_0-\rho_0u_0[u(x)-u_0]=p_0[1-\frac{u_0}{c^2}[u(x)-u_0]=p_0\{1-M_0[M(x)-M_0]\}, \tag{5-3.13}$$

where the Mach numbers $M(x)=u(x)/c$ and $M_0=u_0/c.$ Using Eq. 5-3.3, and the prescribed pressures at the two tube ends, we obtain

$$p_0=c^2(\rho_0-\rho_{\mathrm{L}})+p_L,\quad p(x)u(x)=p_0u_0=p_{\mathrm{L}}u_{\mathrm{L}}=\text{constant} \tag{5-3.14}$$

$$p_0-p_{\mathrm{L}}=\rho_0u_0[u_{\mathrm{L}}-u_0]=M_0[M_L-M_0], \tag{5-3.15}$$

from which, it gives

$$\frac{u_{\mathrm{x}}^2}{c^2}=M_{\mathrm{x}}^2=\frac{p_0+(c^2-1)p_{\mathrm{L}}}{p+(c^2-1)p_{\mathrm{L}}},\qquad \frac{u_{\mathrm{L}}^2}{c^2}=M_{\mathrm{L}}^2=\frac{p_0+(c^2-1)p_{\mathrm{L}}}{p_L+(c^2-1)p_{\mathrm{L}}}=1+\frac{p_0-p_{\mathrm{L}}}{p_Lc^2}. \tag{5-3.16}$$

which shows that the flow is supersonic, since $p_0>p_{\mathrm{L}}$. Now we can obtain the speed, pressure, and mass density of the fluid at any point of tube. In this case, the internal energy in Eq. 5-3.9 will be function of *x* only.

5.3.3 Stable solution by LBM

Now we can use the LBM scheme D1Q3 to deal with the stable problem with the streaming velocity $(0, -\sqrt{2\hat{\varepsilon}}, \sqrt{2\hat{\varepsilon}})$, *which is a function of cell position*. We have known from the performance study of this scheme that its characteristic matrix Eq. 5-1.3 and amplifying matrix Eq. 5-1.5 are unit matrix, i.e., $\widehat{\boldsymbol{V}} = \mathbf{I} = \widetilde{\boldsymbol{A}}$, therefore the transformation $\overline{\boldsymbol{U}}^{(\vartheta+1)} = \overline{\boldsymbol{U}}^{(\vartheta)}$ in Eq. 5-1.6 confirms the initial stable values of variables obtained by Eqs. 5-3.11~16 is stable solution.

The aim of the hand-workable examples given herein is mainly to show that the introduced internal energy variable into LBM equation plays an important role dealing with problems with energy changes in the cell, which caused the difficulty of current LBM theory as mentioned in references cited in introduction of the paper. Therefore, considering page limits, we do not intend to do some numerical examples but leave it for readers to practice it for further developing the theory and proposed method.

6. Conclusion and discussion

To summary the theoretical analysis, we conclude the following contributions of the paper. a) The short introduction on LBM provides the historically important information, which should confirm, based on the author's check, that there have not been found any references presenting the same idea as given in the paper. b) The amended theoretical EDF derived by the H-theorem with Lagrangian multiplier approach includes the mass density, mean velocity, and total internal energy of fluids as three macroscopic parameters, from which the three conservation laws can be directly derived from the BTE without additional small parameter expansions. c) The improved LBM, requiring the internal energy parameter to be updated in each simulation step for general cases, and the updated non-dimensional streaming velocity provides a means to simulate more complex flow problems concerning obvious energy changes in high-speed, compressible flows. The performance study approach is formulated. d) The modified differential BTE includes a new term concerning energy variation allowing external forces and external energy generation source to be considered in the method. e) The hand-workable examples theoretically illustrate the essential characteristics and confirm the proposed improved LBM with the performance study.

The paper is a theoretical document, which have not given complex practical numerical examples, due to pages limited. Author wishes the interested readers may follow the proposed method numerically to tackle some engineering problems from which to further develop this new improved method benefiting to sciences and engineering advances.

Acknowledgement

Author acknowledges the School of Naval Architecture & Ocean Engineering, HUST, providing the finance support managed by Guoxiang Hou, enabling author to visit HUST to tackle LBM. Thanks also are given to Yuehong Qian of Soochow University for providing some references involved in the paper.

References

[1] Landau, L.D., Lifshitz, E.M.: Mechanics. (3rd edn). Butterworth-Heinenann, Oxford (1981)

[2] Hardy,J., Pomeau, Y., De Pazzis, O.: Time evolution of a two-dimensional system, I. Invariant states and time correlation functions. J. Math. Phys. **14**(2), 1746-1759 (1973)

[3] Hardy,J., Pomeau, Y., De Pazzis, O.: Time evolution of a two-dimensional classical lattice system. Phys. Rev Lett. **31**, 276-259 (1973)

[4] Hardy, J, De Pazzis, O., Pomeau, Y.: Molecular dynamics of a lattice gas: transport properties and time correlation functions. Phys. Rev. A**13**, 1949-1961 (1976)

[5] Satoh, A.: Introduction to practice of molecular simulation. Elsevier, London, San Diego (2010)

[6] Huang, K.: Statistical mechanics. (2nd edn). Jhon Wiley & Sons, Chichester (1987, 1963).

[7] Lerner, R.G., Trigg, G.L.: Encylopaedia of physics (2nd ed.). VHC publishers, New York (1991)

[8] Arkeryd, L.: On the Boltzmann equation part I: existence. Arch. Rational Mech. Anal. **45** (1), 1-16 (1972)

[9] Arkeryd, L.: On the Boltzmann equation part II: the full initial value problem. Arch. Rational Mech. Anal. **45** (1), 17-34 (1972)

[10] Crank, J., Nicolson, P.: A practical method for numerical evaluation of solution of partial differential equations of the heat conduction type. Proc. Camb. Phil. Soc. **43**(1), 50-67 (1947)

[11] Hirsch, C.: Numerical computation of internal and external flows, volume 1: fundamentals of numerical discretization. John Wiley & Sons, Chichester (1988).

[12] Inamuro, T., Sturtevant, H.: Numerical study of discrete-velocity gases Phys. Fluids **2**, 2196-2203 (1990)

[13] Bhatnagar, P.L., Gross, E.L., Krook, M.: A model for collision processes in gases. I. Small amplitude processes in charged and neutral one-component systems. Physical Review **94** (3), 511-525 (1954).

[14] Wilson, G.: The life and times of cellular automata. New Scientist 44-47 (1988)
[15] Chopard, B., Droz, M.: Cellular automata modelling of physical systems. Cambridge University Press, London (1998)
[16] McNamara, G., Zanetti, G.: Use of the Boltzmann equation to simulate lattice-gas automata. Physical Review Letters **61**, 2332-2335 (1988)
[17] Broadwell, J.E.: Study of rarefied shear flow by the discrete velocity method. J. Fluid Mech. **19**, 401-414 (1964)
[18] Frisch, U., Hasslacher, B., Pomeau, Y.: Lattice-gas automata for the Navier-Stokes equation. Phys. Rev. Lett. **56** (14), 1505–1508 (1986)
[19] Frisch, U., D'Humieres, D., Hasslacher, B., Lallemand, P., Pomeau, Y., Rivet, J.P.: Lattice gas hydrodynamics in two and three dimensions. Complex Systems **1**, 649-707 (1987)
[20] Higuera, F.J., Jimenez, J.: Boltzmann approach to lattice gas simulations. Europhys. Lett. **9**, 663-668 (1989)
[21] Higuera, F.J., Succi, S., Benzi, R.: Lattice gas dynamics with enhanced collisions. Europhys. Lett. **9**, 345-349 (1989)
[22] Qian, Y.H.: Lattice gas and lattice kinetic theory applied to the Navier-Stokes equations. PhD thesis, University Pierre et Marie Curie, Paris (1990)
[23] Chen, S., Chen, H.D., Martinez, D., Matthaeus, W.: Lattice Boltzmann model for simulation on magnetohydrodynamics. Physics Review Letters **67**, 3376-3379 (1991)
[24] Chen, H., Chen, S., Matthaeus, W.H.: Recovery of the Navier-Stokes equation using a lattice-gas Boltzmann method. Phys. Rev. A **45**, R5339-5342 (1992)
[25] Qian,Y.H., D'Humieres, D., Lallemand, P.: Lattice BGK models for Navier-Stokes equation. Europhysics Letters **17**, 479 (1992)
[26] Qian, Y.H.: Simulating thermodynamics with Lattice BGK models. Journal of Scientific Computing **8,** 231 (1993)
[27] Guo, Z., Shi, B., Wang, N.: Lattice BGK Model for Incompressible Navier-Stokes Equation. Journal Computational Physics **165**, 288-306 (2000)
[28] Guo, Z., Shi, B., Zheng, C.: A coupled lattice BGK model for the Boussinesq equations. Int. J. Numer. Meth. Fluids **39**, 325-342 (2002)
[29] Abe, T.: Derivation of the lattice Boltzmann method by means of the discrete ordinate method for the Boltzmann equation. J. Comp. Phys. **131**, 241-246 (1997)
[30] He, X., Luo, L.S.: A priori derivation of the lattice Boltzmann equation. Phys. Rev. E **55**, 6333-6336 (1997)
[31] He, X., Luo, L.S.: Theory of the lattice Boltzmann method: from the Boltzmann equation to the lattice Boltzmann equation. Phys. Rev. E **56**(6), 6811-6817 (1997)
[32] He, X., Luo, L.S.: Lattice Boltzmann for the incompressible Navier-Stokes equation. J. Stat. Phys. **88**, 927-944 (1997)
[33] Shan, X., He, X.: Discretization of the velocity space in the solution of the Boltzmann equation. Phys. Rev. Lett. **80**, 65 (1998)
[34] Chu, C.K.: Kinetic theoretic description of the formation of a shock wave. Phys. Fluids **8**, 12-21 (1965)
[35] Xu, K., Prendergast, K.H.: Numerical Navier-Stokes solutions from gas kinetic theory. Journal of Computational Physics **114**, 9-17 (1994)
[36] Wolfram, S.: Cellular automation fluids, I. Basic theory. J. Stat. Phys. **45**, 471-526 (1986)
[37] Lavallee, P., Boon, J.P., Noullez, A.: Boundaries in lattice gas flows. Physica D**47,** 233-240 (1991)
[38] Chen, S., Martinez, D., Mei, R.: On boundary conditions in lattice Boltzmann methods. J. Phys. Fluids **8**, 2527-2536 (1996)
[39] Chen, S., Doolen, G.D.: Lattice Boltzmann method for fluid flows. Annual Rev. Fluid Mech. **30**, 329-364 (1998)
[40] Succi, *S*.: The Lattice Boltzmann Equation for Fluid Dynamics and Beyond. Oxford University Press, Oxford. (2001)
[41] Bao, Y. B., Meskas, J.: Lattice Boltzmann Method for Fluid Simulations. appears at webpage https://www.math.nyu.edu (2011)
[42] Zou, Q., He, X.: Pressure and velocity boundary conditions for the lattice Boltzmann. J. Phys. Fluids **9**, 1591-1598 (1997)
[43] Guo, Z. L., Zheng, C. G., Shi, B.C.: Non-equilibrium extrapolation method for velocity and pressure boundary conditions in the lattice Boltzmann method. Chinese Physics **11**(4) 366-374 (2002)
[44] He, X., Doolen, G.: Lattice Boltzmann method on curvilinear coordinate systems: flow around a circular cylinder. Journal of Computational Physics **134**, 306 (1997)
[45] Filippova, O., Hanel, D.: Grid refinement for lattice-BGK models. Journal of computational Physics **147**, 219-228 (1998)

[46] Mei, R., Shyy, W.: On the finite difference-based Boltzmann method in curvilinear coordinates. Journal of Computational Physics **143**, 426 (1998)
[47] Mei, R., Shyy, W., Yu, D., Luo, L.S.: Lattice Boltzmann method for 3-D flows with curved boundary. Journal of Computational Physics **161**, 680-699 (2000)
[48] He, X., Shan, X., Doolen, G.D.: Discrete Boltzmann equation model for nonideal gases. Physical Review E **57,** R13-R16 (1998)
[49] Lee, T., Lin, C.L.: A stable discretization of the lattice Boltzmann equation for simulation of incompressible two-phase flows at high density ration. Journal of Computational Physics **206** (1), 16-47 (2005)
[50] Elton, B.H., Levermore, C.D., Rodrigue, H.: Convergence of convective-diffusive lattice Boltzmann methods. SIAM J. Sci. Comp. **32,** 1327-1354 (1995)
[51] Succi, S., Benzi, R., Higuera, F.: The lattice Boltzmann equation – a new tool for computational fluid dynamics. Physica D**47**, 219-230 (1991)
[52] Noble, D.R., Georgiadis, J.G, Buckius, R.O.: Comparison of accuracy and performance for lattice Boltzmann and finite difference simulation of steady viscous flow. Int. J. Numer. Meth. Fluids **23**, 1-18 (1996)
[53] Sterling, J.D., Chen, S.: Stability analysis of lattice Boltzmann methods. J. Comp. Phys. **123**, 196-206 (1996)
[54] Cao, N., Chen, S., Jin, S., Martinez, D.: Physical symmetry and lattice symmetry in lattice Boltzmann method. Phys. Rev. E **55**, R21-24 (1997)
[55] Koelman, J.M.V.A.: A simple lattice Boltzmann scheme for Navier-Stokes fluid flow. Europhys. Lett. **15**, 603-607 (1991)
[56] Nannelli, F., Succi, S.: The lattice Boltzmann equation on irregular lattices. J. Stat. Phys. **68**, 401-407 (1992)
[57] Amati, G., Succi, S., Benzi, R.: Turbulence channel flow simulation using a coarse-grained extension of the lattice Boltzmann method. Fluid Dyn. Res. **19,** 289-302 (1997)
[58] He, X., Luo, L.S., Dembo, M.: Some progress in lattice Boltzmann method, Part I nonuniform mesh grids. J. Comp. Phys. **129**, 357-363 (1996)
[59] Benzi, R., Succi, S., Vergassola, M.: The lattice Boltzmann equation - theory and application. Phys. Rep. **222,** 145-97 (1992)
[60] Succi, S., Benzi, R., Massaioli, F.: A review of the lattice Boltzmann method. International Journal of Modern Physics C**4** (2), 409-415 (1993)
[61] Rothman, D.H., Zaleski, S.: Lattice gas models of phase separation: interfaces, phase transitions and multiphase flow. Rev. Mod. Phys. **66**, 1417-79 (1994)
[62] Chen, S., Dawso, S.P., Doolen, G.D., Janecky, D.R., Lawniczak, A.: Lattice methods and their applications to reacting systems. Comp. Chem. Eng. **19**, 617-646 (1995)
[63] Qian, Y.H., Succi, S., Orszag, S.A.: Recent advances in lattice Boltzmann computing. Annu. Rev. Comp. Phys. **3**, 195-242 (1995)
[64] Premnath, K., McCracken, M., Abraham, J.: A Review of Lattice Boltzmann Methods for Multiphase Flows Relevant to Engine Sprays. SAE Technical Paper 2005-01-0996, (2005)
[65] Aidum, C.K., Clausen, J.R.: Lattice Boltzmann method for complex flows. Annual Review of Fluid Mechanics **42,** 439-472 (2010)
[66] Seta, T.: Progress in Lattice Boltzmann Method. Japanese Journal of Multiphase flow **24**(4), 427-434 (2010)
[67] Yin, X., Le, G., Zhang, J.: Mass and momentum transfer across solid-fluid boundaries in the lattice-Boltzmann method. Phys. Rev. E Stat. Nonlin. Soft. Matter. Phys. **86**(2 Pt 2): 026701 (2012)
[68] Jahanshaloo, L., Pouryazdanpanah, E., Sidik, N. A. C.: A Review on the application of the lattice Boltzmann method for turbulent flow simulation, Numerical Heat Transfer, Part A: Applications. An International Journal of Computation and Methodology **64** (11), 938-953 (2013)
[69] Djenidi, L.: The lattice Boltzmann method and the problem of turbulence. AIP Conference Proceedings 1648, 030003 (2015)
[70] Che Sidik, N.A., Aisyah Razali, S.: A Review on Lattice Boltzmann Method for Numerical Prediction of Nanofluid Flow. International Review of Mechanical Engineering **7**(7), 1269-1274 (2013)
[71] Che Sidik, N.A, Aisyah Razali, S.: Lattice Boltzmann method for convective heat transfer of nanofluids, Renewable and Sustainable Energy Reviews **38**(C), pages 864-875, Elsevier, London (2014)
[72] Perumal, D.A., Dass, A.K.: A Review on the development of lattice Boltzmann computation of macro fluid flows and heat transfer. Alexandria Engineering Journal **54** (4), 955-971 (2015)
[73] Succi, S., Moradi, N., Greiner, A., Melchionna, S.: Lattice Boltzmann modeling of water-like fluids. Front. Phys. **16** (2014)
[74] Wang, J., Chen, L., Kang, Q., Rahman, S.S.: The lattice Boltzmann method for isothermal micro-gaseous flow and its application in shale gas flow: a review. International Journal of Heat and Mass Transfer **95**, 94-108 (2016)

[75] Yoon, H., Kang, Q., Valocchi, A.J.: Lattice Boltzmann-Based Approaches for Pore-Scale Reactive Transport. Reviews in Mineralogy and Geochemistry **80** (1), 393–431 (2015)
[76] Liu, H., Kang, Q., Leonardi, C.R., Schmieschek, S.M.P., Narvaez Salazar, A.E., Jones, B.D., Williams, J.R., Valocchi, A.J., Harting, J.D.R.: Multiphase lattice Boltzmann simulations for porous media application: a review. Computational Geosciences **20**(4), 777-805 (2016)
[77] Sharma, K.V., Straka, R., Tavares, F.W.: Lattice Boltzmann method for industrial applications. Ind. Eng. Chem. Res. **58**, 16205-16234 (2019)
[78] W. Shao, J. Li, Review of Lattice Boltzmann Method Applied to Computational Aeroacoustics**.** Archives of Acoustics **44**(2), 215–238 (2019)
[79] Carenza, L.N., Gonnella, G., Lamura, A., Negro, G., Tiribocchi, A.: Lattice Boltzmann methods and active fluids. European Physical Journal E **42**, 1-83 (2019)
[80] Wang, H., Yuan, X., Liang, H., Chai, Z., Shi, B.: A brief review of the phase-field-based lattice Boltzmann method for multiphase flows. Capillarity **2**(3), 33-52 (2019)
[81] Li, L., Lu, J., Fang, H., Yin, Z., Wang, T., Wang, R., Fan, X., Zhao, L., Tan, D., Wan, Y.: Lattice Boltzmann method for fluid-thermal systems: status, hotspots, trends and outlook. IEEE Access **8**, 27646-27675 (2020)
[82] Gutowitz, H. (ed): Cellular automata: theory and experiment; proceeding s of a workshop sponsored by the centre for nonlinear studies. Los Alamos National Laboratory, Los Alamos, NM87545, USA, September 9-12, (1989).
[83] Wolf-Gladrow, D.A.: Lattice-gas cellular automata and lattice Boltzmann models, an introduction. Springer, Berlin Heidelberg, New York (2000)
[84] Succi, S.: Lattice Boltzmann equation for complex states of flowing matter. Oxford University Press, Oxford (2018)
[85] Sukop, M., Thorne, D.T.: Lattice Boltzmann Modelling: an introduction for geoscientists and engineers (1st edn). Springer, Berlin Heidelberg, New York (2006)
[86] Mohamad, A.A.: Lattice Boltzmann method: fundamentals and engineering applications with computer codes (1st & 2nd edns). Springer, Berlin Heidelberg, New York (2011 / 2019)
[87] Mohamad, A.A. (author), Yang, D. (translator): Lattice Boltzmann method: fundamentals and engineering applications with computer codes (in Chinese). Electronic Industry Press, China (2015)
[88] Guo, Z., Shu, C.: Lattice Boltzmann method and its applications in engineering (Advances in Computational Fluid Dynamics). World Scientific Publishing Company, London (2013)
[89] Stoer, J., Bulirsch, B.: Introduction to numerical analysis. Springer, Berlin Heidelberg, New York (1992).
[90] Huang, H., Sukop, M., Lu, X.: Multiphase lattice Boltzmann methods: theory and application, John Wiley & Sons, Chichester (2015)
[91] Krüger, T., Kusumaatmaja, H., Kuzmin, A., Shardt, O., Silva, G., Viggen, E.M.: The lattice Boltzmann method, principles and practice. Springer, Berlin Heidelberg, New York (2017)
[92] Montessori, A., Falcucci, G.: Lattice Boltzmann modeling of complex flows in engineering applications. Morgan & Claypool Publishers, San Rafael, CA, 94901, USA (2018)
[93] Akker, H. (Ed.): Lattice Boltzmann modeling for chemical engineering, Volume 55. Academic Press, London, New York (2020)
[94] Bolton, D.C., Schwartz, B., Shreedharan, S.: Lattice Boltzmann methods, pp1-55. appears at webpage https://www.ems.psu.edu (2020)
[95] He, Y., Wang, Y., Li, Q.: Lattice Boltzmann method: Theory and Applications (in Chinese). Science Press, Beijing (2009)
[96] Guo, Z., Zheng, Z.: Theory and applications of lattice Boltzmann method (in Chinese). Science Press, Beijing (2009)
[97] Wang, H., Li, X.: Applications of lattice Boltzmann method in partial differential equations of soliton waves (in Chinese). Science Press, Beijing (2017)
[98] Begum, R., Basit, M.A.: Lattice Boltzmann Method and its Applications to Fluid Flow Problems. Euro. J. Sci. Research **22,** 216-231 (2008)
[99] Wagner, A.J.: A practical introduction to the lattice Boltzmann method. Department of Physics, North Dakota State University, Fargo, March 2008, at http://www.physics.ndsu.nodak.edu/wagner/LB.html.
[100] Chen, L.: Lattice Boltzmann for flow and transport phenomena. appears at webpage https://gr.xjtu.edu.cn/web/lichennht08 (2018)
[101] Swift, M.R., Osborn, W.R., Yeomans, J.M.: Lattice Boltzmann simulation of nonideal fluids. Phys. Rev. Lett. **75**, 830-833 (1995)
[102] Swift, M.R., Orlandini, S.E., Osborn, W.R., Yeomans, J.M.: Lattice Boltzmann simulation of liquid-gas and binary-fluid systems. Phys. Rev. E **54**, 5041-5052 (1996)
[103] Nadiga, B.T., Zaleski, S.: Investigations of a two-phase fluid model. Eur. J. Mech. B/fluids **15**, 885-896 (1996)

[104] He, X., Chen, S., Doolen, G.D.: A novel model for the lattice Boltzmann method in compressible limit. Journal of Computational Physics, Elsevier **146** (1), 282-300 (1998)
[105] Jacob, J., Malaspinas, O., Sagaut, P.: A new hybrid recursive regularized Bhatnagar-Cross-Krook collision model for lattice Boltzmann method-based large eddy simulation. J. Turbul. **19**(11), 1051-76 (2018)
[106] Feng, Y., Boivin, P., Jacob, J., Sagaut, P.: Hybrid recursive regularized thermal lattice Boltzmann model for high subsonic compressible flows. J. Comput. Phys. **394**, 82-99 (2019)
[107] Renard, F., Feng, Y., Boussuge, J.-F., Sagaut, P.: Improved compressible hybrid lattice Boltzmann method on standard lattice for subsonic and supersonic flows. Computers and Fluids **219**, 104867 (2021)
[108] Shan, X.: Central-moment-based Galilean-invariant multiple-relation-time collision model. Phys. Rev. E **100**(4), 043308 (2019)
[109] Wilde, D., Krämer, A., Küllmer, K., Foysi, H., Reith, D.: Multistep lattice Boltzmann methods: theory and applications. Int. J. Numer. Methods Fluids **90**(3), 156-169 (2019)
[110] Saadat, M.H., Bösch, F., Karlin, I.V.: Lattice Boltzmann model for compressible flows on standard lattices: variable Prandtl number and adiabatic exponent. Phys. Rev. E **99**(1), 013306 (2019)
[111] Feng, Y.-L., Tao, W.-Q., Sagaut, P.: Regularized thermal lattice Boltzmann method for natural convection with large temperature differences. Int. J. Heat Mass Transf. **125**, 1379-91 (2018)
[112] Wissocq, G., Sagaut, P., Boussuge, J.F.: An extended spectral analysis of the lattice Boltzmann method: model interactions and stability issues. J. Comut. Phys. **380**, 311-33 (2019)
[113] Fung, Y.C.: A first course in continuum mechanics (3rd edn). Prentice-Hall, London (1977)
[114] Xing, J.T.: Fluid-solid interaction dynamics, theory, variational principles, numerical methods, and applications. Academic Press, Elsevier, London (2019)
[115] Xing, J.T.: Fluid-solid interaction dynamics, theory, variational principles, numerical methods, and applications. Higher Education Press, Beijing (2021)
[116] Xing, J.T., Price, W. G.: A power flow analysis based on continuum dynamics. Proc. R. Soc. Lond. *A* **455**, 401-435 (1999)
[117] Xing, J.T., Price, W. G.: The energy flow equation of continuum dynamics. In IUTAM Symposium on Statistical Energy Analysis, (eds. F. Fahy & W. G. Price), pp. 83-94. Kluwer academic publishers, Netherlands (1999)
[118] Xing, J.T.: Energy flow theory of nonlinear dynamical systems with applications, Springer, Berlin Heidelberg, New York (2015)
[119] Xing, J.T.: Generalised energy conservation law of chaotic phenomena. Acta Mech Sin **35**(6), 1257-1268 (2019) http://doi.org/10.1007/s10409-019-00886-7
[120] Qin, L., Qin, H., Xing, J.T.: Energy flow characteristics of friction-induced nonlinear vibrations in a water-lubricated bearing-shat coupled system. Acta Mech Sin 37(4), 679-704 (2020) http://doi.org/10.1007/s10409-020-01047-x
[121] Zhang, F.: The Schur complement and its applications, Springer, Berlin Heidelberg, New York (2005)

Figures

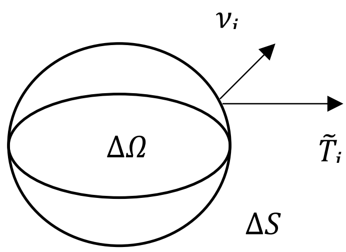

Figure 1

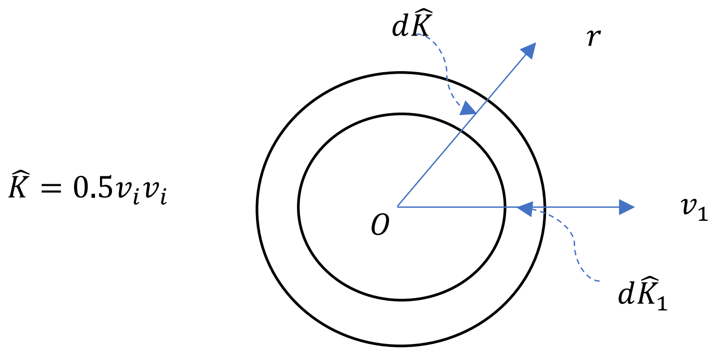

Figure 2

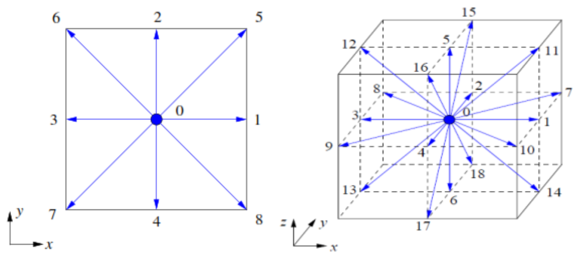

a) b)

Figure 3

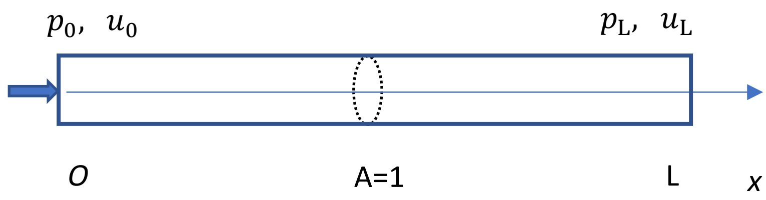

Figure 4